Available online www.jocpr.com
Journal of Chemical and Pharmaceutical Research, 2021, 13(9):3-16

Research Article

ISSN: 0975-7384
CODEN(USA): JCPRC5

Quantum Chemical Prediction of Redox Potential Apply to Phenolic Derivatives

Chabi Doco R*, Kpota Houngue MTA, Koudjina S, Kpotin GA, Atohoun YGS

Department of Chemistry, Laboratory of Theoretical Chemistry and Molecular Spectroscopy, Cotonou, Benin

ABSTRACT

Reliable prediction of oxidation-reduction potential in phenolic compounds involves determination of quantum and molecular descriptors. In this work, the redox potential of set of thirty-one (31) molecules was determined using seven different quantum descriptors and one molecular descriptor. The calculations, performed at the SWN/6-31G, HF/6-31G and AM1 theory level allowed us to establish the Quantitative Structure-Property Relationship (QSPR) analysis of substituted phenols that can predict redox potential with confidence level of over 95%.

Keywords: Redox potential; Theory level; Phenols; QSPR

INTRODUCTION

Phenolic compounds are of great interest because of their involvement in biological and industrial processes. They have important biological activities (anticancer, antioxidant, anti-cardiovascular and anti-inflammatory). Several studies have shown that hydroxyl groups of these compounds are essential in free radicals trapping. Recent theoretical works have shown existence of several quantum descriptors that can predict antioxidant properties of these bioactive molecules [1-5]. In addition, the work of Steenken, et al., Jovanovic et al., have shown that redox potential is an important experimental parameter for elucidating and comparing antioxidant powers of phenol derivatives as well as that of hydroxyl groups on the flavonoids ring system [4,5].

The goal of our work is to develop models for predicting redox potential by SWN/6-31G, HF/6-31G and AM1 theory level. For this, appropriate descriptors will be selected from a set of seven quantum descriptors and a molecular descriptor, taking into account only those that are highly correlated with redox potential while being independent of each other. The results of this work will make it possible to establish and validate by a statistical method efficient QSPR models [2].

MATERIALS AND METHODS

Thirty-one (31) phenolic compounds whose experimental values of redox potential E are known were selected in the literature and form the structural basis of our study. These phenolic compounds are divided in two groups or sets: the training set containing 21 molecules (≈ 2/3 of the base molecules) and the test set containing 10 molecules (≈ 1/3 of the basis molecules). The choice of molecules for the constitution of groups is arbitrary. Molecules are codified Fi in order to simplify their notations [3] (Table 1).

Table 1: Structure of phenolic compounds

Code	Compounds	Code	Compounds
F_1	4-NO_2	F_{17}	2-OCH_3-4-CH_3
F_2	4-CN	F_{18}	3, 4-$(CH_3O)_2$
F_3	4-I	F_{19}	3, 4,5-$(CH_3O)_3$
F_4	4-$COCH_3$	F_{20}	Sesamol
F_5	4-COOH	F_{21}	2-OH-4-COOH
F_6	4-H	F_{22}	2, 6-$(CH_3O)_2$
F_7	4-Br	F_{23}	2, 3-$(OH)_2$
F_8	4-Cl	F_{24}	2,3-$(OH)_2$-5-$COOCH_3$
F_9	4-F	F_{25}	3,4-Dihydroxycinnamic acid
F_{10}	Tyrosine	F_{26}	2-OH
F_{11}	3-OH-4-$COCH_3$	F_{27}	2-OH-4-CH_3
F_{12}	4-CH_3	F_{28}	α-Tocopherol
F_{13}	3,5-$(CH_3O)_2$	F_{29}	4-OH
F_{14}	3-OH-5-OCH_3	F_{30}	4-NH_2
F_{15}	3-OH	F_{31}	4-$(CH_3)_3$
F_{16}	4-OCH_3		

All molecules were optimized using SWN/6-31G, HF/6-31G and AM1 theory level as implemented in GAUSSIAN 09 program. Two software's XLSTAT and EXCEL have been used, according to their specificities, to conduct statistical analysis of the results and to draw the graph [4-6].

The principle of linear regression is to model a quantitative dependent variable Y through a linear combination of p quantitative explanatory variables X_1, X_2……X_p. The deterministic model is written as:

$$Y= \beta_0+\beta_1 X_1+ \beta_2 X_2+ \ldots\ldots. +\beta_p X_p+ \varepsilon$$

Where β_i are coefficients of the regression and ε the model error. The choice of quantum descriptors is based on two fundamental criteria [7].

Criterion 1

By nature, the dependence of Y on X_i is assumed to be linear. For this, the absolute value of the linear correlation coefficient between the property Y and the variables X_i must be greater than 0.50.

$|R| \geq 0.50$

Criterion 2

the different samples Y_i are supposed to be independent of each other. For two descriptors i and j to be independent, the partial correlation coefficient (a_{ij}) between them must be strictly less than 0.70 [8].

$a_{ij}<0.70$

The predictive power of a model is also based on Tropsha criteria. If the three fifths (3/5) of the criteria are verified then the model has a good predictive power.

Criterion 1: $R_{ext}^2>0.70$;

Criterion 2: $Q_{ext}^2>0.60$;

Criterion 3: $(R_{ext}^2-R_0^2)/(R_{ext}^2)<0.1$ and $0.85<k<1.15$

Criterion 4: $(R_{ext}^2-R_0'^2)/(R_{ext}^2)<0.1$ and $0.85<k'<1.15$

Criterion 5: $|R_{ext}^2-R_0^2| \leq 0.30$

Normality tests have also been performed to verify the quality of the confidence interval obtained. These are Shapiro-Wilk and Durbin-Watson tests. The different expressions and the notations of the quantum descriptors used are gathered in Table 2.

Table 2: Quantum descriptors used expressed in electron volt (eV)

Quantum descriptors	Energy HOMO	Energy LUMO	Energy gap	Electronegativity	Hardness	Molless	Electrophily indice
Expressions	E_{HOMO}	E_{LUMO}	E_{LUMO}-E_{HOMO}	χ=(IP+EA)/2	η=(IP-EA)/2	S=1/(2η)	$\omega=\chi^2/2\eta$

The HOMO and LUMO orbitals obtained on each 31 set of molecules ($F_1 \ldots F_{31}$) have been used to calculate the different parameters of the quantum descriptors [9-11]. This orbitals means have to make the quantum descriptor choice easier under the caster of the chemical selective methods (Figure 1).

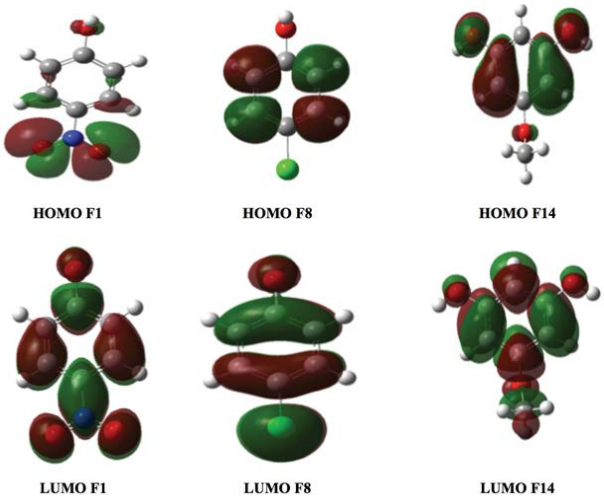

Figure 1: A few illustrations of HOMO and LUMO molecular orbitals as the tools to calculate the quantum parameters, which make the choice of quantum descriptors, show on the molecules F_1, F_8 and F_{14}

RESULTS AND DISCUSSION

Choice of Quantum Descriptors

Calculated values of quantum descriptors at SWN/6-31G, HF/6-31G and AM1 theory level for molecules of the learning set and their redox potentials identified in the literature are summarized (Tables 3-5).

Table 3: Redox potential values of the quantum and molecular descriptors at SWN/6-31G level of approximation for the learning set

Code	Quantum descriptors							Molecular descriptor	Redox potential
	E_{HOMO}	E_{LUMO}	Gap	χ	η	S	ω	nOH	E
F_1	-0.36	-0.07	0.29	0.2	0.15	2.94	0.94	0	1.23
F_2	-0.34	-0.05	0.29	0.18	0.16	2.78	0.11	0	1.17
F_3	-0.32	-0.04	0.28	0.16	0.15	2.94	0.1	0	1.09
F_4	-0.32	-0.04	0.28	0.16	0.15	2.94	0.1	0	1.06
F_5	-0.32	-0.05	0.27	0.17	0.15	2.94	0.11	0	1.04
F_6	-0.32	-0.04	0.28	0.16	0.15	2.94	0.1	0	0.97
F_7	-0.32	-0.04	0.28	0.16	0.15	2.94	0.1	0	0.96
F_8	-0.32	-0.03	0.29	0.16	0.16	2.78	0.09	0	0.94
F_9	-0.32	-0.03	0.29	0.16	0.16	2.78	0.09	0	0.93
F_{10}	-0.32	0.04	0.28	0.16	0.16	2.78	0.08	0	0.89

F_{11}	-0.32	-0.04	0.28	0.16	0.15	2.94	0.09	1	0.89
F_{12}	-0.32	0.04	0.28	0.15	0.16	2.78	0.08	0	0.87
F_{13}	-0.3	0.05	0.25	0.14	0.16	2.78	0.07	0	0.85
F_{14}	-0.31	0.04	0.27	0.15	0.16	2.78	0.08	1	0.84
F_{15}	-0.3	0.05	0.25	0.14	0.15	2.94	0.08	1	0.81
F_{16}	-0.32	0.04	0.28	0.16	0.16	2.78	0.09	0	0.73
F_{17}	-0.29	0.05	0.24	0.13	0.15	2.94	0.07	0	0.68
F_{18}	-0.29	0.04	0.25	0.14	0.15	2.94	0.08	0	0.67
F_{19}	-0.3	0.04	0.26	0.14	0.15	2.94	0.08	0	0.66
F_{20}	-0.29	0.03	0.26	0.14	0.14	3.13	0.08	0	0.62
F_{21}	-0.31	-0.05	0.27	0.14	0.16	2.78	0.07	1	0.6

Table 4: Redox potential values of the quantum and molecular descriptors at HF/6-31G level of approximation for the learning set

Code	Quantum descriptors							Molecular descriptor	Redox potential
	E_{HOMO}	E_{LUMO}	Gap	χ	η	S	ω	nOH	E
F_1	-0.29	-0.06	0.23	0.18	0.12	4.17	0.14	0	1.23
F_2	-0.29	-0.06	0.23	0.18	0.12	4.17	0.14	0	1.17
F_3	-0.29	-0.06	0.23	0.18	0.12	4.17	0.14	0	1.09
F_4	-0.29	-0.06	0.23	0.18	0.12	4.17	0.14	0	1.06
F_5	-0.3	-0.08	0.22	0.19	0.11	4.55	0.16	0	1.04
F_6	-0.33	-0.08	0.25	0.21	0.13	3.85	0.17	0	0.97
F_7	-0.29	-0.09	0.2	0.19	0.1	5	0.18	0	0.96
F_8	-0.3	-0.08	0.22	0.19	0.11	4.55	0.16	0	0.94
F_9	-0.32	-0.08	0.24	0.2	0.12	4.17	0.17	0	0.93
F_{10}	-0.3	-0.08	0.22	0.19	0.11	4.55	0.16	0	0.89
F_{11}	-0.31	-0.07	0.24	0.19	0.12	4.17	0.15	1	0.89
F_{12}	-0.31	-0.06	0.25	0.19	0.13	3.85	0.14	0	0.87
F_{13}	-0.31	-0.07	0.24	0.19	0.12	4.17	0.15	0	0.85
F_{14}	-0.31	-0.09	0.22	0.2	0.11	4.55	0.18	1	0.84
F_{15}	-0.32	-0.09	0.23	0.22	0.12	4.17	0.2	1	0.81
F_{16}	-0.3	-0.09	0.21	0.2	0.11	4.55	0.18	0	0.73
F_{17}	-0.29	-0.08	0.21	0.19	0.11	4.55	0.16	0	0.68
F_{18}	-0.3	-0.09	0.21	0.2	0.11	4.55	0.14	0	0.67
F_{19}	-0.34	-0.08	0.26	0.21	0.13	3.85	0.17	0	0.66
F_{20}	-0.29	0.03	0.26	0.14	0.14	3.13	0.08	0	0.62
F_{21}	-0.31	-0.05	0.27	0.14	0.16	2.78	0.07	1	0.6

Table 5: Redox potential values of the quantum and molecular descriptors at AM1 level for the learning set

Code	Quantum descriptors							Molecular descriptor	Redox potential
	E_{HOMO}	E_{LUMO}	Gap	χ	η	S	ω	nOH	E
F_1	-0.39	-0.05	0.34	0.22	0.17	2.94	0.94	0	1.23
F_2	-0.37	-0.02	0.35	0.2	0.18	2.78	0.11	0	1.17
F_3	-0.35	-0.01	0.34	0.18	0.17	2.94	0.1	0	1.09
F_4	-0.35	-0.01	0.34	0.18	0.17	2.94	0.1	0	1.06
F_5	-0.35	-0.02	0.33	0.19	0.17	2.94	0.11	0	1.04
F_6	-0.35	-0.01	0.34	0.18	0.17	2.94	0.1	0	0.97

F_7	-0.35	-0.01	0.34	0.18	0.17	2.94	0.1	0	0.96
F_8	-0.35	0	0.35	0.18	0.18	2.78	0.09	0	0.94
F_9	-0.35	0	0.35	0.18	0.18	2.78	0.09	0	0.93
F_{10}	-0.34	0.01	0.35	0.17	0.18	2.78	0.08	0	0.89
F_{11}	-0.35	-0.01	0.34	0.17	0.17	2.94	0.09	1	0.89
F_{12}	-0.34	0.01	0.35	0.17	0.18	2.78	0.08	0	0.87
F_{13}	-0.33	0.02	0.35	0.16	0.18	2.78	0.07	0	0.85
F_{14}	-0.34	0.01	0.35	0.17	0.18	2.78	0.08	1	0.84
F_{15}	-0.33	0.01	0.34	0.16	0.17	2.94	0.08	1	0.81
F_{16}	-0.35	0	0.35	0.18	0.18	2.78	0.09	0	0.73
F_{17}	-0.32	0.02	0.34	0.15	0.17	2.94	0.07	0	0.68
F_{18}	-0.32	0.01	0.33	0.16	0.17	2.94	0.08	0	0.67
F_{19}	-0.33	0.01	0.34	0.16	0.17	2.94	0.08	0	0.66
F_{20}	-0.32	0	0.32	0.16	0.16	3.13	0.08	0	0.62
F_{21}	-0.34	-0.02	0.36	0.16	0.18	2.78	0.07	1	0.6

The calculated values of the quantum descriptors at SWN/6-31G, HF/6-31G and AM1 theory level of the learning set and their redox potentials identified in the literature are summarized (Tables 6-8).

Table 6: Redox potential values of the quantum and molecular descriptors at SVWN/6-31G level of the test set

Code	Quantum descriptors							Molecular descriptor	Redox potential
	E_{HOMO}	E_{LUMO}	Gap	χ	η	S	ω	nOH	E
F_{22}	-0.36	-0.07	0.29	0.2	0.15	2.94	0.94	0	0.58
F_{23}	-0.34	-0.05	0.29	0.18	0.16	2.78	0.11	2	0.58
F_{24}	-0.32	-0.04	0.28	0.16	0.15	2.94	0.1	2	0.56
F_{25}	-0.32	-0.04	0.28	0.16	0.15	2.94	0.1	1	0.54
F_{26}	-0.32	-0.04	0.33	0.17	0.15	2.94	0.11	1	0.53
F_{27}	-0.32	-0.04	0.34	0.16	0.15	2.94	0.1	1	0.52
F_{28}	-0.32	-0.04	0.34	0.16	0.15	2.94	0.1	1	0.46
F_{29}	-0.32	-0.03	0.35	0.16	0.16	2.78	0.09	1	0.48
F_{30}	-0.32	-0.03	0.35	0.16	0.16	2.78	0.09	0	0.41
F_{31}	-0.31	0.04	0.35	0.15	0.16	2.78	0.08	0	0.36

Table 7: Redox potential values of the quantum and molecular descriptors at SVWN/6-31G level of the test

Code	Quantum descriptors							Molecular descriptor	Redox potential
	E_{HOMO}	E_{LUMO}	Gap	χ	η	S	ω	nOH	E
F_{22}	-0.3	-0.13	0.17	0.22	0.09	5.55	0.27	0	0.58
F_{23}	-0.31	-0.1	0.21	0.21	0.11	4.55	0.2	2	0.58
F_{24}	-0.31	-0.12	0.19	0.22	0.11	4.55	0.22	2	0.56
F_{25}	-0.3	-0.08	0.22	0.19	0.11	4.55	0.16	1	0.54
F_{26}	-0.31	-0.12	0.21	0.22	0.11	4.55	0.22	1	0.53
F_{27}	-0.3	-0.13	0.17	0.22	0.09	5.55	0.27	1	0.52
F_{28}	-0.3	-0.13	0.17	0.22	0.09	5.55	0.27	1	0.46
F_{29}	-0.31	-0.13	0.18	0.22	0.09	5.55	0.27	1	0.48
F_{30}	-0.31	-0.12	0.19	0.22	0.11	4.55	0.2	0	0.41
F31	-0.31	-0.11	0.2	0.21	0.1	5	0.22	0	0.36

Table 8: Redox potential values of the quantum and molecular descriptors at AM1 level of the test set

Code	Quantum descriptors							Molecular descriptor	Redox potential
	E_{HOMO}	E_{LUMO}	Gap	χ	η	S	ω	nOH	E
F_{22}	-0.4	-0 .05	0.3	0.2	0.2	3	1	0	0.58
F_{23}	-0.4	-0.02	0.4	0.2	0.2	3	0	2	0.58
F_{24}	-0.4	-0.01	0.3	0.2	0.2	3	0	2	0.56
F_{25}	-0.4	-0.01	0.3	0.2	0.2	3	0	1	0.54
F_{26}	-0.4	-0.02	0.3	0.2	0.2	3	0	1	0.53
F_{27}	-0.4	-0.01	0.3	0.2	0.2	3	0	1	0.52
F_{28}	-0.4	-0.01	0.3	0.2	0.2	3	0	1	0.46
F_{29}	-0.4	0	0.4	0.2	0.2	3	0	1	0.48
F_{30}	-0.4	0	0.4	0.2	0.2	3	0	0	0.41
F_{31}	-0.3	0.01	0.4	0.2	0.2	3	0	0	0.36

Verification of the dependency of variables: Two thirds (2/3) of the molecules (21 molecules) from the database were used for the development of models (training set and the 10 remaining will be used for the verification of models [12-16] (Table 9).

Criteria Verification 1

Table 9: Selection of quantum descriptors by criterion 1

	SVWN/6-31G		HF/6-31G		AM1	
Equations	**Correlation coefficient linear lRl**	**Descriptor rejected if lRl<0.50**	**Correlation coefficient linear lRl**	**Descriptor rejected if lRl<0.50**	**Correlation coefficient linear lRl**	**Descriptor rejected if lRl<0.50**
E and E_{HOMO}	0.72	Retained	0.64	Retained	0.84	Retained
E and E_{LUMO}	0.56	Retained	0.56	Retained	0.62	Retained
E and Gap	0.09	Rejected	0.23	Rejected	0.05	Rejected
E and χ	0.79	Rejected	0.64	Retained	0.86	Retained
E and η	0.04	Rejected	0.13	Rejected	0.07	Rejected
E and S	0.12	Rejected	0.34	Rejected	0.09	Rejected
E and ω	0.43	Rejected	0.28	Rejected	0.49	Rejected
E and nOH	0.37	Rejected	0.32	Rejected	0.27	Rejected

Analysis of the results in Table 9 allows us to remember that for the SVWN/6-31G level of approximation, descriptors selected are: energy of the LUMO (E_{LUMO}) and electronegativity (χ).

Analysis of the results in Table 9 allows us to remember that for the HF/6-31G level of approximation, descriptors selected are: energy of the LUMO (E_{LUMO}) and electronegativity (χ).

Analysis of the results in Table 9 allows us to remember that for the AM1 level of approximation, descriptors selected are: Energy of the HOMO (E_{HOMO}), energy of LUMO (E_{LUMO}) and electronegativity (χ) [17].

Application of criterion 2: Definitive selection of quantum descriptors.

The results of definitive selection of quantum descriptors at SWN/6-31G, HF/6-31G and AM1 level are shown in Table 10.

Table 10: Definitive selection of quantum descriptors at SWN/6-31G level

Correlation between:	Coefficient	Descriptors independent if<0.70
E_{HOMO} and E_{LUMO}	0.79	Dependent
E_{HOMO} and χ	-0.83	Independent
E_{LUMO} and χ	-0.68	Independent

Analysis of the results in Table 10 shows that the descriptors: energy of the LUMO (E_{LUMO}) and the energy of HOMO (E_{HOMO}) are dependent on each other. They cannot belong to the same group. Hence one needs to consider two groups of predictive quantum descriptors [18]. The two groups of quantum descriptors are as follows (Table 11).

Group 3: LUMO energy (E_{LUMO}) and electronegativity (χ)

Group 4: HOMO energy (E_{HOMO}) and electronegativity (χ)

Table 11: Definitive selection of quantum descriptors at HF/6-31G level

Correlation between	Coefficient	Descriptors independent if<0.70
E_{HOMO} and E_{LUMO}	0.79	Dependent
E_{HOMO} and χ	-0.71	Independent
E_{LUMO} and χ	-0.88	Independent

Analysis of the results in Table 11 shows that the descriptors: energy of the LUMO (E_{LUMO}) and the energy of HOMO (E_{HOMO}) are dependent on each other. They cannot belong to the same group. Hence one needs to consider two groups of predictive quantum descriptors [19] (Table 12). The two groups of quantum descriptors are as follows:

Group 5: LUMO energy (E_{LUMO}) and electronegativity (χ)

Group 6: HOMO energy (E_{HOMO}) and electronegativity (χ)

Table 12: Definitive selection of quantum descriptors at AM1 level

Correlation between	Coefficient	Descriptors independent if< 0.70
E_{HOMO} and E_{LUMO}	0.84	Dependent
E_{HOMO} and χ	-0.95	Independent
E_{LUMO} and χ	-0.82	Independent

Analysis of the results in Table 12 shows that the descriptors: energy of the LUMO (E_{LUMO}) and the energy of HOMO (E_{HOMO}) are dependent on each other. They cannot belong to the same group. Hence one needs to consider two groups of predictive quantum descriptors. The two groups of quantum descriptors are as follows:

Group 1: LUMO energy (E_{LUMO}) and electronegativity (χ)

Group 2: HOMO energy (E_{HOMO}) and electronegativity (χ)

QSPR models of antioxidant properties: From learning set and predictive descriptors selected, we established a QSPR model of the redox potential E. To choose the group that will be used to establish the regression equation of the QSPR model, the Fisher coefficients of the two groups will be compared and then the most significant group in Fisher's sense will be used [20].

Model regression equation: The Fisher coefficients for groups 3 and 4 are provided by the ANOVA tables in Tables 13 and 14.

Table 13: ANOVA table of SWN/6-31G level quantum descriptors for group 3

	DS	SC	MSC	F1	P-value
Regression residual total	2	0.51	0.42	17.23	0.000011
	18	0.61	0.12		
	20	0.113			

Table 14: ANOVA table of SWN/6-31G level quantum descriptors for group 4

	DS	SC	MSC	F2	P-value
Regression residual total	2	0.84	0.24	92.46	0.000015
	18	0.72	0.01		
	20	0.153			

Analysis of the results in Tables 13 and 14 shows that the Fisher coefficient (F2) of group 4 is greater than the Fisher coefficient (F1) of group 4: F1<F2; this means that the group 4 regression equation will be more significant than that of group 3. Group 4 quantum descriptors can therefore be meaningful in redox potential QSPR model establishing at SWN/6-31G level. The results of the multi-linear regression obtained from descriptors of group 4 are shown in Table 15.

The Fisher coefficients for groups 5 and 6 are provided by the ANOVA tables in Tables 15 and 16.

Table 15: ANOVA table of AM1 level quantum descriptors for group1

	DS	SC	MSC	F1	P-value
Regression residual total	2	16313,77	32,62,753	42,61,446	0.0003
	16	29023,16	22,32,551		
	18	45336,93			

Analysis of the results shows that the Fisher coefficient (F2) of group 6 is greater than the Fisher coefficient (F1) of group 5: F1<F2; this means that the group 6 regression equation will be more significant than that of group 5. Group 6 quantum descriptors can therefore be meaningful in redox potential QSPR model establishing at HF/6-31G level [21]. The results of the multi-linear regression obtained from descriptors of group 6 are shown in Table 16.

Table 16: ANOVA table of AM1 level quantum descriptors for group 2

	DS	SC	MSC	F2	P-value
Regression residual total	2	11056,65	22,11,329	0,8378	0,0546
	16	34310,79	26,39,292		
	18	45367,44			

The Fisher coefficients for groups 1 and 2 are provided by the ANOVA tables in Tables 17 and 18.

Table 17: ANOVA table of AM1 level quantum descriptors for group 1

	DS	SC	MSC	F1	P-value
Regression residual total	2	0.47	0.23	26.32	0.000005
	18	0.16	0.01		
	20	0.63			

Table 18: ANOVA table of AM1 level quantum descriptors for group 2

	DS	SC	MSC	F2	P-value
Regression residual total	2	0.48	0.24	29.64	0.000002
	18	0.14	0.01		
	20	0.63			

Analysis of the results in Tables 17 and 18 shows that the Fisher coefficient (F2) of group 2 is greater than the Fisher coefficient (F_1) of group 1: F_1<F_2; this means that the group 2 regression equation will be more significant than that of group 1. Group 2 quantum descriptors can therefore be meaningful in redox potential QSPR model

establishing at AM1 level. The results of the multi-linear regression obtained from descriptors of group 2 are shown in Table 19.

Table 19: Regression coefficients value of group 3 for model

Constants	Coefficients	Ecart-type	Test t	P-value
	-2.21	0.67	-1.46	0.15
E_{LUMO}	-1.3	2.47	-0.45	0.65
χ	10.24	4.42	2.37	0.09

Regression equation of the model is: E=-2, 21-1, 3 E_{LUMO}+10, 24 χ

ANOVA table of the model that allowed analysis of the variance. This ANOVA table indicates that the p-value (0.000011) is less than α=0.05 showing that the equation model regression is significant in redox potential predicting (Table 20).

Table 20: Regression coefficients values of group 6 for model

Constants	Coefficients	Standard deviation	Test t	P-value
	-28.44	16.71	-2.35	0.003
E_{LUMO}	52.01	40.83	0.36	0.072
χ	-71.26	24.56	-0.13	0.894

Regression equation of the model is: E=-28.44-52.01E_{LUMO}+71.26χ. The p-value (0.000002) is less than α=0.05 showing that the equation Model regression is significant in redox potential predicting (Table 21).

Table 21: Regression coefficients values of group 1 for model

Constants	Co-efficients	Standard deviation	Test t	P-value
	-1.12	0.76	-1.46	0.15
E_{LUMO}	-1.93	4.27	-0.45	0.65
χ	7.7	4.42	1.73	0.09

Regression equation of the model is: E=-1.12 -1.93 ELUMO+7.70 χ

ANOVA table of the model that allowed analysis of the variance is that of Table 7. This ANOVA table indicates that the p-value (0.000002) is less than α=0.05 showing that the equation Model regression is significant in redox potential predicting.

Contribution of quantum descriptors in the prediction of redox potential E

The analysis of the results in Table 19-21 shows that

According to absolute values of the t-test in Table 19, the importance of the quantum descriptors of the SVWN/6-31G level in the model is in the following ascending order: E_{LUMO}<χ; Contribution calculations show that LUMO energy (E_{LUMO}) contributes 10.54 in the prediction of the redox potential and the electronegativity (χ) has a contribution of 84.04. It is clear that electronegativity (χ) is the main descriptor predictive of the redox potential of these phenolic derivatives.

According to absolute values of the t-test in Table 20, the importance of the quantum descriptors of the HF/6-31G level in the model is in the following ascending order: χ<E_{LUMO} Contribution calculations show that LUMO energy (E_{LUMO}) contributes 73.46 in the prediction of the redox potential and the electronegativity (χ) has a contribution of 26.53. It is clear that energy (E_{LUMO}) is the main descriptor predictive of the redox potential of these phenolic derivatives.

According to absolute values of the t-test in Table 21, the importance of the quantum descriptors of the AM1 level in the model is in the following ascending order: E_{LUMO}< χ

Contribution calculations show that LUMO energy (E_{LUMO}) contributes 20.64 in the prediction of the redox potential and the electronegativity (χ) has a contribution of 79.35. It is clear that electronegativity (χ) is the main descriptor predictive of the redox potential of these phenolic derivatives.

Statistical Parameters of the Model

Results for statistical parameters are shown in Table 22.

Table 22: Statistical parameters of the model

Levels	n	R	R_2	R_{2aj}	S	F	FIT
SVWN/6-31G	21	0.47	0.22	0.43	0.078	17.23	0.67
HF/6-31G	21	0.98	0.96	0.83	0.087	4.26	0.76
AM1	21	0.97	0.95	0.93	0.095	29.64	0.96

The analysis of the results in Table 22 shows that

For the SVWN/6-31G theory level,

The value of correlation coefficient R obtained (R=0.47) is lower than 1. This means that the redox potential is too weakly correlated with the variables energy of LUMO (E_{LUMO}) and the electronegativity (χ).

The coefficient of determination obtained R2 indicates that the model does not have an explanatory power on the redox potential and that the descriptors have no effect on property explained.

Of all the above, the model cannot predict the potential. The x model is rejected.

For HF/6-31G theory level,

Analysis of data in Table 22 shows that redox potential is strongly correlated with quantum descriptors selected because of R-value of 0.98. In addition, 98% of experimental variance of redox potential is explained by the descriptors of the model. We can say that the model is validated and can be used as a model to predict the redox potential of molecules.

For AM1 theory level,

Data shows that redox potential is strongly correlated with quantum descriptors selected because of R-value of 0.97. In addition, 95% of experimental variance of redox potential is explained by the descriptors of the model 1. We can say that the model is validated and can be used as a model to predict the redox potential of molecules.

LOO Internal Validation of the Model,

The internal validation method applied in this study is cross-validation by omission of one molecule (in English Leave-One-Out: LOO). Cross validation LOO has been applied to the molecules of the learning game (Table 23).

Table 23: Statistical parameters of the LOO internal and external validation of the model

Interne	n	PRESS	Q^2_{Loo}	S_{press}	
	21	0.087	0.95	0.203	
Extern	n	R_{2ext}	PRESS	Q_{2ext}	S_{PRESS}
	10	0.97	0.33	0.98	0.53

The analysis of the results in Table 23 indicates that,

The model has a very high predictive power (Q_{Loo}^2=0.95) because 95% of molecules in the learning game have their predicted redox potential.

The model has high predictive power (Q^2_{ext}=0.98) because 98.1% of the test set molecules has their predicted redox potential. In addition 97% of the experimental variance of the redox potential is explained by the quantum descriptors of the model (Table 24).

Table 24: Statistical parameters of the LOO internal and external validation of the model

Interne	N	PRESS	Q^2_{Loo}	S_{press}	
	19	0.082	0.92	0.103	
Extern	N	R_{2ext}	PRESS	Q^2_{ext}	S_{PRESS}
	10	0.99	0.19	0.94	0.31

The analysis of the results in Table 24 indicates that

The model has a very high predictive power (Q_{Loo}^2=0.92) because 92% of molecules in the learning game have their predicted redox potential.

The model has high predictive power (Q^2_{ex}t=0.94) because 94.1% of the test set molecules has their predicted redox potential. In addition 99% of the experimental variance of the redox potential is explained by the quantum descriptors of the model.

Verification of Tropsha's criteria for the model

At HF/6-31G level

- R_{ext}^2=0.85>0.70;
- Q^2_{ext}=0.71>0.60;
- $(R_{ext}^2-R_0^2)/(R_{ext}^2)$=0.13>0.10 et 0.85< k<1.15;
- $(R_{ext}^2-R_0'^2)/(R_{ext}^2)$=0.03<0.10 et 0.85< k<1.15;
- $| R_{ext}^2-R_0^2 |$=1.33>1.15.

We note that four of the five (3/5) the Tropsha criteria are verified. The model is therefore very efficient in the prediction of the redox potential E.

At HF/6-31G level

(1) R_{ext}^2=0.99>0.70;

(2) Q^2_{ext}=0.94>0.60;

(3) $(R_{ext}^2-R_0^2)/(R_{ext}^2)$=0.05<0.10 et 0.85< k<1.15;

(4) $(R_{ext}^2-R_0'^2)/(R_{ext}^2)$=0.05<0.10 et 0.85<k<1.15;

(5) $| R_{ext}^2-R_0^2 |$=1.25>1.15.

We note that four of the five (4/5) the Tropsha criteria are verified. The model is therefore very efficient in the prediction of the redox potential E.

Normality Tests of the Model

At HF/6-31G level,

The results provided by the XLSTAT software are: Shapiro-Wilk test (Epred)

This test gives the following results: w=0.837; p-value=0.172; α=0.05

Test Interpretation: Since the calculated p-value is greater than the alpha threshold significance level (0.172>0.05), it is concluded that the predicted values of redox potential by the model follow a normal distribution.

Durbin-Watson test (residues),

This test gives the following results: U=0.787; p-value=0.266; α=0.05

Interpretation of the test: Since the calculated p-value is greater than the alpha threshold level of significance (0.787>0.05), it is concluded that the residues are not self-correlated. As result, they do not contain information that can influence the prediction of the model.

From different analyses of statistical tests, we can retain that the mode 1 established on the quantum descriptors: LUMO energy (E_{LUMO}) and the electronegativity (χ) is validated and very powerful in the prediction of the redox

potential. The regression equation of the prediction can be summarized as follows:

Prediction equation of the redox potential of model 1

$E=-28.44-52.01E_{LUMO}+71.26\chi$

n =31; R=0.98; R^^2=0.96; R_{aj}^^2=0.83; S=0.087; F=4.26; FIT=0.76

At AM1 Level,

The results provided by the XLSTAT software are: Shapiro-Wilk test (E_{pred})

This test gives the following results: w=0.931; p-value=0.194; α=0.05

Test interpretation: Since the calculated p-value is greater than the alpha threshold significance level (0.194>0.05), it is concluded that the predicted values of redox potential by the model follow a normal distribution.

Durbin-Watson test (residues),

This test gives the following results: U=0.578; p-value=0.456; α=0.05

Interpretation of the test: Since the calculated p-value is greater than the alpha threshold level of significance (0.456>0.05), it is concluded that the residues are not self-correlated. As result, they do not contain information that can influence the prediction of the model.

From different analyses of statistical tests, we can retain that the model 2 established on the quantum descriptors: LUMO energy (E_{LUMO}) and the electronegativity (χ) is validated and very powerful in the prediction of the redox potential. The regression equation of the prediction can be summarized as follows:

Prediction equation of the redox potential of model 2

$E=-1.12-1.93\ E_{LUMO}+7.70\ \chi$

n=31; R=0.97; R^2=0.95; R_{aj}^2=0.93; S=0.095; F=29.64; FI =0.96

Correlation between calculated potential E_{pred} and experimental E_{exp}

At HF/6-31G Level,

The curve in Figure 2 shows a strong linear correlation between predicted and experimental redox potentials. This graph confirms that the model 1 is validated and is very efficient in predicting redox potentials for this type of phenolic compounds (Figure 2).

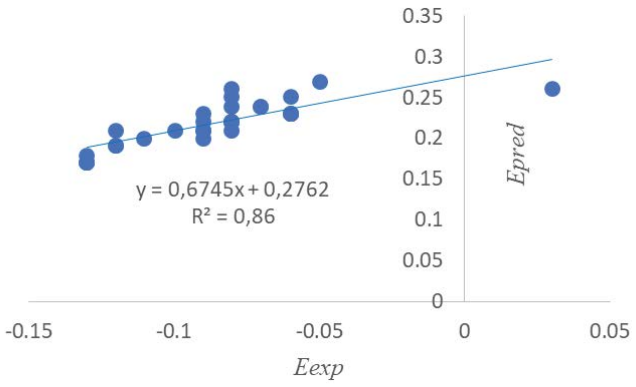

Figure 2: A plot of calculated values (E_{pred}) vs. experimental values (E_{exp}) by using equation

n=31; R=0.98; R^2=0.96; R_{aj}^2=0.83; S=0.087; F=4.26; FIT=0.76

At AM1 Level,

The curve shows a strong linear correlation between predicted and experimental redox potentials. This graph confirms that the model 2 is validated and is very efficient in predicting redox potentials for this type of phenolic compounds (Figure 3).

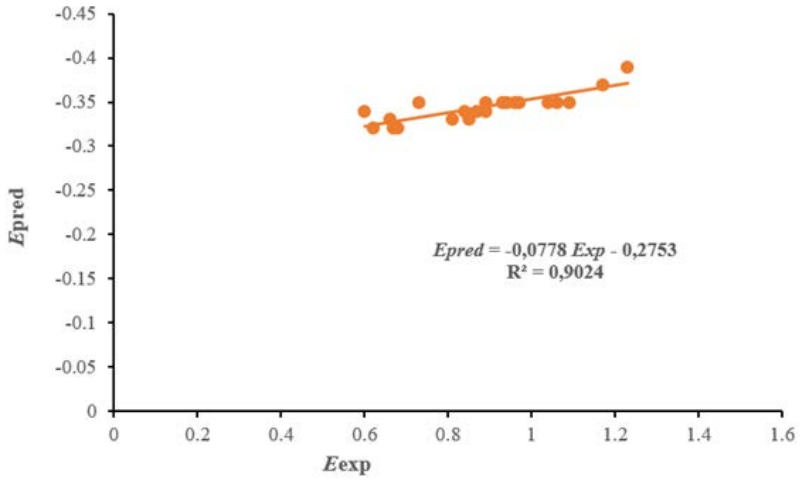

Figure 3: A plot of calculated values (Epred) vs. experimental values (Eexp) by using equation

E=-1.12-1.93 E_{LUMO}+7.70 χ, with n=31, and R^2=0.95.

Comparison of QSPR models for the prediction of redox potential established during this study

The purpose is to make a comparative study of the four QSPR models established in this study in order to obtain a classification of performance of these four models. Fisher coefficient is used to compare overall significance of the QSPR models established. The results are shown in Table 25.

Table 25: Fisher coefficients of established models

Models	Fisher coefficients (F)
Model 1 : HF/6-31G	4.26
Model 2 : (AM1)	29.64

Analysis of data in Table 25 shows that the most significant QSPR model in sense of Fisher is model 2 established because of its Fisher coefficient, which is the highest (F=29.64). On other hand, the least significant model is the model 1 established from the quantum descriptors at the HF/6-31G level of approximation because having the lowest coefficient of Fisher (F=4.26). We obtain this decreasing order of significance according to established models: Model 2>Model 1.

CONCLUSION

The QSPR methodology and quantum chemical methods were used to establish predictive models of redox potential of 31 phenolic derivatives. Two groups of quantum descriptors have been identified according to the basic criteria generally used. The results showed that the quantum descriptors: LUMO energy (E_{LUMO}) and electronegativity (χ) correlated strongly with the redox potential of molecules. The statistical analysis allowed us to find two models explained by two equations: E=-1.12-1.93 E_{LUMO}+7.70 χ and E=-28.44-52.01E_{LUMO}+71.26χ obtained respectively from AM1 and HF/6-31G, which predict the redox potential with 95% and 98% confidence level respectively.

ACKNOWLEDGEMENTS

The calculations have been performed on the LACTHESMO Equipment of Professor Jean-Baptiste MENSAH at the University of Abomey-Calavi in Benin, and on PPMS at University of Lorraine. The authors would like to thank especially the PPMS (Pôle Messin de Modelisation et de Simulation) for providing us HPC resources.

REFERENCES

[1] Rice-Evans CA, Diplock AT. *Free Radic Biol Med*. **1993**; 15, 77- 96.

[2] Cadenas E, Packer L. *J Phy Chem*. **1996**.

[3] Rice-Evans C A, Packer L. *Free Radic Biol Med*. **1998**.

[4] Steenken S, Neta P. *J Phys Chem*. **1982**; 86, 3661-3667.

[5] Jovanovic SV, Tosic M, Simic M G. *J Phys Chem*. **1991**; 95, 10824-10827.

[6] Shertzer HG, Tabor MW, Hogan ITD, et al. *Arch Toxicol*. **1996**; 70, 830-834.

[7] Van Acker SABE, de Groot MJ, Van den Berg D, et al. *Chem Res Toxicol.* **1996**; 9, 1305-1312.

[8] Cao G, Sofic E, Prior R L. *Free Radi Biol Med*. **1997**; 22, 749-760.

[9] Burton GW, Le Page Y, Gabe EJ, et al. *J Am Chem Soc*. **1980**; 102, 7791-7792.

[10] Burton GW, Doba T, Gabe EJ, et al. J Am Chem Soc. 1985; 107, 7053-7056.

[11] Doba T, Burton GW, Ingold KU. J Am Chem Soc. 1983; 105, 6505-6506.

[12] Frisch MJ, Trucks GW, Schlegel HB, et al. *Free Radi Biol Med*. **2013**.

[13] XLSTAT. *Addinsoft*. **2014**.

[14] Partie de Microsoft Office. *Professionnel Plus*. **2013**.

[15] Lien EJ, Ren S, Bui HH, et al. *Free Radi Biol Med*. **1999**; 26, 285-294.

[16] Van Acker SABE, Koymans LMH, Bast A. *Free Radi Biol Med*. **1993**; 15, 311-328.

[17] Rice-Evans CA, Packer L. *J Phys Chem*. **1998**.

[18] Chabi Doco R, Kpota Houngue MTA, Gaston KA, et al. *J Chem Pharma Res*. **2017**; 9(5), 231-236.

[19] Steenken S, Neta P. *J Phys Chem*. **1982**; 86, 3661-3667.

[20] Jovanovic SV, Tosic M, Simic MG. *J Phy Chem*. **1991**; 95, 10824-10827

[21] Burton GW, Hughes L, Ingold KU. *J Am Chem Soc*. **1983**; 105, 5950-5951.

International Research Journal of Pure & Applied Chemistry

22(7): 19-34, 2021; Article no.IRJPAC.72000
ISSN: 2231-3443, NLM ID: 101647669

QSPR/QSAR Modelling of the Antioxidant Properties of Some Flavonoids

R. Chabi Doco[1*], M. T. A. Kpota Houngue[1], Urbain A. Kuevi[1] and Y. G. S. Atohoun[1]

[1]Laboratory of Theoretical Chemistry and Molecular Spectroscopy (LACTHESMO), University of Abomey-Calavi, 03 BP 3409 Cotonou, Benin.

Authors' contributions

This work was carried out in collaboration among all authors. All authors read and approved the final manuscript.

Article Information

DOI: 10.9734/IRJPAC/2021/v22i730418
Editor(s):
(1) Dr. Farzaneh Mohamadpour, University of Sistan and Baluchestan, Iran.
Reviewers:
(1) Valerio Benedetti, University of Turin, Italy.
(2) Jigisha Anand, Deemed To Be University, India.
Complete Peer review History: https://www.sdiarticle4.com/review-history/72000

Original Research Article

Received 10 June 2021
Accepted 15 August 2021
Published 25 August 2021

ABSTRACT

Several methods exist when seeking to experimentally evaluate the antioxidant properties of a natural bioactive substance. In the case of flavonoids, the methods used are mainly based on the experimental determination of the percentage of inhibition (IC50) or the redox potential (E).
In the present work, a prediction study of the redox potential *E* and the inhibitory concentration *LogIC50* was carried out, using the AM1 and HF/6-311G(d,p) method.
At the end of this study, three (03) QSPR models were validated and retained, one (01) for the prediction of the redox potential and four (02) for the prediction of the inhibitory concentration :

- **The Redox Prediction Model**, developed at the AM1 approximation level, for which 96.43 of the experimental variance is explained by the descriptors :

$E = -0,29 + 0,22E_{Homo} + 0,11E_{Lumo} - 0,05\bar{\omega}^{-}$

- **The Inhibitory Concentration Prediction Models**, developed at the AM1 level, for which 96.35P of the experimental variance is explained by the descriptors :

$LogIC_{50} = -4,92 + 11,37E_{Homo} + 34,36E_{Lumo} + 0,67\bar{\omega}^{-}$

- **The Inhibitory Concentration Prediction Model**, developed at the HF/6-311G level (d, p), for which 99.96P of the experimental variance is explained by the descriptors. $LogIC_{50} = 62,40 + 80,25\ E_{Homo} - 28,44E_{lumo} + 52,01S - 71,26\ \eta - 6,11\mu$

**Corresponding author: E-mail: titiwan1980@gmail.com;*

The development of these QSPR models represents a significant advance in predicting the antioxidant properties of bioactive molecules such as flavonoids based on descriptors calculated by quantum chemical methods.

Keywords: Antioxidant; properties; QSAR/QSPR; quantum descriptors.

1. INTRODUCTION

The field of investigation is vast when it comes to experimentally evaluating the antioxidant properties of flavonoids. The methods used are mainly based on the experimental determination of the percentage inhibition (IC50) or the redox potential (E).

Indeed, several results published in the literature have shown that experimental parameters such as redox potential and inhibitory concentration allow to evaluate the antioxidant powers of bioactive molecules [1,2,3,4,5] (Jorgensen et *al.* 1999; Volikakis et *al.* 2000; Yamamura, 2003 and and Dragan AMI et *al.* 2017).

In the present work, QSAR/QSPR models for predicting antioxidant properties were developed. The aim is to find a linear relationship that will predict the experimental parameters E or IC50 as a function of quantum descriptors such as : electronic affinity (EA), ionisation energy (EI), hardness (η), softness (S), electronegativity (χ), electrophilic index (ω), energy (HOMO), energy (LOMO), energy gap (HOMO-LUMO), electrophilic index (ω), dipole moment (μ***,*** electron donor ($\overline{\omega}^-$) and electron acceptor ($\overline{\omega}^+$), used in our previous studies.

From the results obtained, the redox potential (E) and the inhibitory concentration (IC50) of the flavonoids will be predicted and consequently their antioxidant power.

2. MATERIALS AND METHODOLOGY

2.1 Materials

In our work, 29 flavonoids with known experimental redox potential (E) and inhibitory concentration (IC50) values were selected as the structural basis for study. These flavonoids are classified into two groups or series: the learning series with 19 molecules (≈ *2⁄3* of the base molecules) and the test series with 10 molecules (≈ *1⁄3* of the base molecules). The choice of molecules for the constitution of the groups is arbitrary. These molecules are coded M_i in order to simplify their notations.

The molecules of the learning set will be used to develop predictive models of redox potential and inhibitory concentration from quantum descriptors, and those of the test set for validation of the developed models. The experimental values of the redox potential and the inhibitory concentration of the molecules are taken from the literature [6].

2.2 Methodology

For the determination of the quantum descriptors on which the prediction models of the redox potential E and the inhibitory concentration IC50 of the studied molecules were developed, different levels of calculations were used. These are : AM1 and HF/6-311G (d, p). These levels of theory were chosen in view of the size of the molecules and the different quantum parameters to be evaluated.

2.2.1 Statistical analysis

All molecules were optimised using the GAUSSIAN 09 program**.** Two software packages were used, according to their specificities, to perform the statistical analysis of the results and to plot the graph, i.e. XLSTAT and MATLAB**.** The choice of the quantum descriptors is based on two fundamental criteria.

Criterion 1: By nature, the dependence of *Y* on X_i is assumed to be linear. Therefore the absolute value of the linear correlation coefficient between the property *Y* and the variables X_i must be greater than 0.50: **|R| ≥0.50**

Criterion 2: The different samples Y_i are assumed to be independent of each other. For two descriptors to be independent, the partial correlation coefficient (a_{ij}) between these two descriptors i and j must be strictly less than 0.70 : $a_{ij} < 0.70$

Table 1. Structure of the flavonoids studied

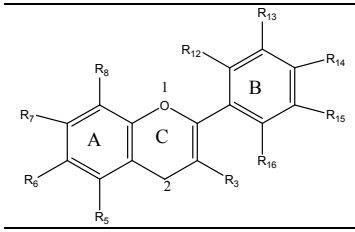

Basic structure of flavonoids											
Molecules	**C2**	**R3**	**R5**	**R6**	**R7**	**R8**	**R12**	**R13**	**R14**	**R15**	**Names**
M1	C	H	OH	H	OH	H	H	H	OH	OH	Epigallo catechin
M2	C	H	OH	H	OH	H	H	OH	OH	OH	Epigallocatechingallate
M3	C	Gallate	OH	H	OH	H	H	OH	OH	H	Epicatechin gallate
M4	C	Gallate	OH	H	OH	H	H	OH	OH	OH	Gallocatechin gallate
M5	C	Gallate	OH	H	OH	H	H	H	OH	OH	Catechin gallate
M6	C	OH	OH	H	OH	H	H	OH	OH	H	- Catechin
M7	C	OH	OH	H	OH	H	H	H	OH	OH	- Epicatechin
M8	C	OH	OH	H	OH	H	H	H	OH	OH	+ Epicatechin
M9	C	OH	OH	H	OH	H	H	OH	OH	H	+ Catechin
M10	C=O	OH	OH	H	OH	H	H	H	4-(2, 3, 4-trihydroxybutyl)-2-methoxyphenol		Silibinin
M11	C=O	H	H	OH	H	OH	H	OH	H	H	Luteolin
M12	C=O	H	H	OH	H	OH	H	H	H	H	Wogonin
M13	C=O	H	H	OH	H	OH	H	H	H	H	Apigenin
M14	C=O	OH	OH	H	H	OH	H	OH	H	H	Fustin
M15	C=O	OH	OH	OH	H	OH	H	H	H	H	Naringenin
M16	C=O	H	H	H	H	OH	H	H	H	H	Daidzein
M17	C=O	H	H	H	Glucose	H	H	H	OH	H	Daidzin
M18	C=O	H	H	H	OH	Glucose	H	H	OH	H	Puerarin
M19	C	OH	OH	H	OH	H	H	OH	OH	OH	Gallocatechin
M20	C=O	OH	OH	H	OH	H	H	OH	OH	OH	Myricetin
M21	C=O	OH	OH	H	OH	H	H	OH	H	H	Quercetin
M22	C=O	OH	H	H	OH	H	H	OH	H	H	Fisetin
M23	C=O	OH	OH	H	OH	H	H	H	H	H	Kaempferol

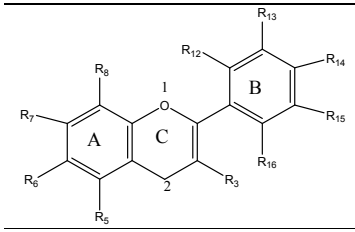

Basic structure of flavonoids

Molecules	C2	R3	R5	R6	R7	R8	R12	R13	R14	R15	Names
M24	C=O	OH	OH	H	OH	H	OH	H	H	H	Morin
M25	C=O	OH	OH	H	OH	H	H	H	H	H	Galangin
M26	C=O	Rutinose	H	H	H	H	H	OH	OH	H	Rutin
M27	C=O	Glucose	OH	H	OH	H	H	OH	H	H	Hyperoside
M28	C=O	OH	OH	OH	H	H	H	H	H	H	Baïcalein
M29	C=O	OH	OH	Glucose	H	H	H	H	H	H	Baïcalin

Table 2. Molecules in the learning and test series

Molecules in the learning series		Molecules in the test series	
N°	**Name of the molecules**	**N°**	**Name of the molecules**
M1	-(2R, 3R) Epigallocatechin	M20	Myricetin
M2	-(2R, 3R)-Epigallocatechin gallate	M21	Quercetin
M3	-(2S, 3R) -Gallocatechin gallate	M22	Fisetin
M4	(-) -(2S, 3R) -catechin gallate	M23	Kampferol
M5	-(2R, 3R)-Epicatechin gallate	M24	Morin
M6	(+) -(2S, 3S)-Epicatechin	M25	Galangin
M7	(-) -(2R, 3R) -Epicatechin	M26	Rutin
M8	(-) -(2S, 3R)-Catechin	M27	Hyperoside
M9	(+) -(2S, 3R)-Catechin	M28	Baicalein
M10	Silibinin	M29	Baicalin
M11	Luteolin		
M12	Wogonin		
M13	Apigenin		
M14	Fustin		
M15	Naringenin		
M16	Daidzein		
M17	Daidzin		
M18	Puerarin		
M19	-(2S, 3R) -Gallocatechin		

Chart 1. Quantum descriptors used. Debye (D)*; Electron-volt (eV)*

Quantum descriptors	Rating	Expression	Unit
Dipole moment	**μ**	-	(D)
Energy of the HOMO	E_{Homo}	-	*(eV)*
Energy from the LUMO	E_{Lumo}	-	*(eV)*
Electronic affinity	AE	$AE = -E_{Lumo}$ [12]	*(eV)*
Ionisation energy	IE	$IE = -E_{Homo}$ ([13]	*(eV)*
GAP (HOMO-LUMO)	Gap	Gap = $E_{Lumo} - E_{Homo}$	*(eV)*
Electronegativity	χ	$\chi = \frac{(IP + EA)}{2}$ [14]	*(eV)*
Hardness.	η	$\eta = \frac{(IP - EA)}{2}$ [15]	*(eV)*
Softness	S	$S = \frac{1}{2\eta}$ [16]	$(eV)^{-1}$
Electrophilic Index	ω	$\omega = \frac{\chi^2}{2\eta}$ [17]	*(eV)*
Donor electron power	$\bar{\omega}^-$	$\bar{\omega}^- = \frac{(3.EI+AE)^2}{16(EI-AE)}$ [18]	*(eV)*
Electron acceptor power	$\bar{\omega}^+$	$\bar{\omega}^+ = \frac{(EI+3.AE)^2}{16(EI-AE)}$ [19]	*(eV)*

The predictive power of a model is also based on the Tropsha criteria. If the three fifths (3/5) of the criteria are verified then the model has a good predictive power. Normality tests were also carried out to verify the quality of the confidence interval obtained. These are the Shapiro-Wilk and Durbin-Watson tests.

2.2.2 Theoretical descriptors

These are quantum descriptors calculated by quantum chemical methods. Chart 1 shows the quantum descriptors used in this study [7,8,9,10,11] [20-24].

2.2.3 Contribution of an explanatory variable to the prediction of a property

The contribution of an explanatory variable X_i noted C_{X_i} to the prediction of a property of *Y* is based on the statistical parameter t_test which indicates the significance of an explanatory variable in a model [25].

$$C_{X_i} = \frac{|t\_test(X_i)|}{\Sigma|(t\_test(X_i)|} \times 100$$

The contribution is expressed as a percentage (%), where $|t\_test(X_i)|$, the absolute value of the t_test of the variable X_i ; $\Sigma|(t\_test(X_i)|$ the sum of the absolute values of the t_test of all the variables X_i of the model. The higher C_{X_i} is, the greater the contribution of the explanatory variable X_i in the model developed [26].

3. RESULTS AND DISCUSSION

In Tables 3 to 6, the values of the calculated quantum descriptors and the values of the redox potential E and the inhibitory concentration IC50 of the molecules of the training and test series are recorded.

3.1 Selection of Quantum Descriptors for the Prediction of the *LogIC50* Inhibitory Concentration

The results for the final selection of the predictive quantum descriptors for the *LogIC50* inhibitory concentration are reported in Tables 8 and 9.

The results in Table 8 allow us to consider two groups of predictive quantum descriptors of *LogIC50* for the AM1 level:

- **Group 3**: LUMO Energy ($_{ELumo}$), HOMO Energy (*EHomo*) and Electron Donor Power ($\bar{\omega}^-$) ;
- **Group 4:** Energy of the HOMO (*EHomo*), Electron Acceptance Power ($\bar{\omega}^+$) and Electron Donor Power ($\bar{\omega}^-$).

The analysis of Table 9 reveals that the quantum descriptors selected for the prediction of *LogIC50 at* the HF/6-311G level (d, p) are: EHomo, $_{ELumo}$, S, η, χ and μ. These quantum descriptors allow us to consider two groups:

- **Group 5**: HOMO energy (*EHomo*), LUMO energy ($_{ELumo}$), Softness (*S*), Hardness (η) and Density (μ);
- **Group 6:** LUMO energy ($_{ELumo}$), Softness (S), Hardness (η), Electronegativity (χ), and Dipole moment (μ).

Table 3. Values of the quantum descriptors calculated at the AM1 level and the experimental values of the redox potential E and the inhibitory concentration IC50 of the training series

Code	Quantum descriptors										Experimental descriptors	
	EHomo	$_{ELumo}$	*Gap*	*χ*	*η*	*S*	*ω*	*μ*	$\bar{\omega}^+$	$\bar{\omega}^-$	*E*	*LogIC50*
M1	-0 .33	-0 .00	0.33	0.17	0.17	2.94	0.09	3.34	0.02	0 .02	-0.030	-4.98
M2	-0 .33	-0 .02	0.31	0.18	0.16	3.13	0.10	2.61	0.03	0 .21	0.020	-5.07
M3	-0 .33	-0 .00	0.33	0.17	0.17	2.94	0.09	3.12	0.02	0 .02	0.030	-4.68
M4	-0 .33	-0 .02	0.31	0.18	0.16	3.13	0.10	4.11	0.03	0 .21	0.080	-4.72
M5	-0 .33	-0 .01	0.32	0.17	0.16	3.13	0.09	0.57	0.03	0 .20	0.105	-4.64
M6	-0 .33	-0 .01	0.32	0.17	0.16	3.13	0.09	1.21	0.03	0 .20	0.280	-4.86
M7	-0 .32	-0 .01	0.31	0.17	0.16	3.13	0.09	2.78	0.02	0 .19	0.180	-4.03
M8	-0 .33	-0 .00	0.33	0.17	0.17	2.94	0.09	3.30	0.02	0 .02	0.185	-4.23
M9	-0 .33	-0 .00	0.33	0.17	0.17	2.94	0.09	1.56	0.02	0 .02	-0.060	-5.20
M10	-0 .33	-0 .01	0.32	0.17	0.16	3.13	0.09	4.13	0.02	0 .20	0.080	-4.70
M11	-0 .33	-0 .04	0.29	0.19	0.15	3.33	0.12	3.03	0.04	0 .23	0.180	-4.58
M12	-0 .33	-0 .03	0.30	0.18	0.15	3.33	0.11	2.87	0.04	0 .22	0.360	-
M13	-0 .34	-0 .03	0.31	0.19	0.16	3.13	0.11	2.35	0.04	0 .22	0.500	-
M14	-0 .33	-0 .02	0.31	0.18	0.16	3.13	0.10	2.43	0.03	0 .21	0.132	4.18
M15	-0 .34	-0 .02	0.32	0.18	0.16	3.13	0.10	2.64	0.03	0 .21	0.590	-
M16	-0 .32	-0 .02	0.30	0.17	0.15	3.33	0.10	1.98	0.03	0 .20	0.500	-
M17	-0 .32	-0 .02	0.30	0.17	0.15	3.33	0.10	3.03	0.03	0 .20	0.538	-
M18	-0 .33	-0 .03	0.31	0.18	0.16	3.13	0.10	1.40	0.04	0 .21	0.540	-
M19	-0 .33	-0 .00	0.33	0.17	0.17	2.94	0.09	1.06	0.02	0 .02	-0.030	-4.53

Table 4. Values of the quantum descriptors calculated at AM1 and the experimental values of the redox potential E and the inhibitory concentration IC50 of the test series

Code	Quantum descriptors										Experimental descriptors	
	E_{Homo}	E_{Lumo}	Gap	χ	η	S	ω	μ	$\bar{\omega}^{+}$	$\bar{\omega}^{-}$	E	$LogIC_{50}$
M20	-0 .32	-0 .04	0.28	0.18	0.14	3.57	0.12	1.06	0 .04	0 .22	-0.035	-4.80
M21	-0 .32	-0 .04	0.28	0.18	0.14	3.57	0.12	2.14	0 .04	0 .22	-0.020	-4.96
M22	-0 .32	-0 .04	0.28	0.18	0.14	3.57	0.12	2.39	0 .04	0 .22	-0.010	-4.89
M23	-0 .32	-0 .04	0.28	0.18	0.14	3.57	0.12	0.49	0 .04	0 .22	0.040	-4.89
M24	-0 .31	-0 .03	0.28	0.18	0.14	3.57	0.12	1.91	0 .04	0 .21	0.080	-5.00
M25	-0 .32	-0 .04	0.28	0.18	0.14	3.57	0.12	2.20	0 .04	0 .22	0.082	-4.60
M26	-0 .31	-0 .03	0.28	0.18	0.14	3.57	0.12	2.95	0 .04	0 .21	0.082	-4.52
M27	-0 .32	-0 .03	0.29	0.18	0.15	3.33	0.11	1.62	0 .04	0 .34	0.092	-4.42
M28	-0 .35	-0 .03	0.32	0.19	0.16	3.13	0.11	2.95	0 .04	0 .23	0.102	-4.29
M29	-0 .32	-0 .03	0.29	0.18	0.15	3.33	0.11	4.62	0 .04	0 .21	0.450	-4.01

Table 5. Values of the quantum descriptors calculated at the HF/6-311G level (d, p) and the experimental values of the redox potential E and the inhibitory concentration IC50 of the training set

Code	Quantum descriptors										Experimental descriptors	
	E_{Homo}	E_{Lumo}	Gap	χ	η	S	ω	μ	$\bar{\omega}^{+}$	$\bar{\omega}^{-}$	E	$LogIC_{50}$
M1	-0.29	-0.06	0.23	0.18	0.12	4.17	0.14	2.06	0.06	0.24	-0.030	-4.98
M2	-0.29	-0.06	0.23	0.18	0.12	4.17	0.14	2.61	0.06	0.24	0.020	-5.07
M3	-0.29	-0.06	0.23	0.18	0.12	4.17	0.14	2.45	0.06	0.24	0.030	-4.68
M4	-0.29	-0.06	0.23	0.18	0.12	4.17	0.14	1.02	0.06	0.24	0.080	-4.72
M5	-0.30	-0.08	0.22	0.19	0.11	4.55	0.16	2.73	0.08	0.27	0.105	-4.64
M6	-0.33	-0.08	0.25	0.21	0.13	3.85	0.17	8.10	0.08	0.27	0.280	-4.86
M7	-0.29	-0.09	0.20	0.19	0.10	5.00	0.18	4.21	0.10	0.29	0.180	-4.03
M8	-0.30	-0.08	0.22	0.19	0.11	4.55	0.16	3.68	0.08	0.27	0.185	-4.23
M9	-0.32	-0.08	0.24	0.20	0.12	4.17	0.17	3.70	0.08	0.28	-0.060	-5.20
M10	-0.30	-0.08	0.22	0.19	0.11	4.55	0.16	7.85	0.06	0.27	0.080	-4.70
M11	-0.31	-0.07	0.24	0.19	0.12	4.17	0.15	4.39	0.07	0.26	0.180	-4.58
M12	-0.31	-0.06	0.25	0.19	0.13	3.85	0.14	3.77	0.06	0.25	0.360	-
M13	-0.31	-0.07	0.24	0.19	0.12	4.17	0.15	3.35	0.07	0.26	0.500	-
M14	-0.31	-0.09	0.22	0.20	0.11	4.55	0.18	3.02	0.10	0.30	0.132	4.18

Code	Quantum descriptors										Experimental descriptors	
	E_{Homo}	E_{Lumo}	Gap	χ	η	S	ω	μ	$\bar{\omega}^{+}$	$\bar{\omega}^{-}$	E	$LogIC_{50}$
M15	-0.32	-0.09	0.23	0.22	0.12	4.17	0.20	3.91	0.09	0.30	0.590	-
M16	-0.30	-0.09	0.21	0.20	0.11	4.55	0.18	2.35	0.10	0.29	0.500	-
M17	-0.29	-0.08	0.21	0.19	0.11	4.55	0.16	4.30	0.08	0.27	0.538	-
M18	-0.30	-0.09	0.21	0.20	0.11	4.55	0.14	2.83	0.10	0.24	0.540	-
M19	-0.34	-0.08	0.26	0.21	0.13	3.85	0.17	10.45	0.08	0.29	-0.030	-4.53

Table 6. Values of the quantum descriptors calculated at the HF/6-311G level (d, p) and the experimental values of the redox potential E and the inhibitory concentration IC50 of the test series

Code	Quantum descriptors										Experimental descriptors	
	E_{Homo}	E_{Lumo}	Gap	χ	η	S	ω	μ	$\bar{\omega}^{+}$	$\bar{\omega}^{-}$	E	$LogIC_{50}$
M20	-0.30	-0.13	0.17	0.22	0.09	5.55	0.27	4.12	0.11	0.32	-0.035	-4.80
M21	-0.31	-0.10	0.21	0.21	0.11	4.55	0.20	3.25	0.14	0.36	-0.020	-4.96
M22	-0.31	-0.12	0.19	0.22	0.11	4.55	0.22	4.76	0.08	0.27	-0.010	-4.89
M23	-0.30	-0.08	0.22	0.19	0.11	4.55	0.16	4.54	0.14	0.36	0.040	-4.89
M24	-0.31	-0.12	0.21	0.22	0.11	4.55	0.22	1.55	0.18	0.39	0.080	-5.00
M25	-0.30	-0.13	0.17	0.22	0.09	5.55	0.27	1.97	0.18	0.39	0.082	-4.60
M26	-0.30	-0.13	0.17	0.22	0.09	5.55	0.27	1.82	0.18	0.36	0.082	-4.52
M27	-0.31	-0.13	0.18	0.22	0.09	5.55	0.27	3.91	0.14	0.36	0.092	-4.42
M28	-0.31	-0.12	0.19	0.22	0.11	4.55	0.20	1.81	0.13	0.34	0.102	-4.29
M29	-0.31	-0.11	0.20	0.21	0.10	5.00	0.22	5.27	0.11	0.32	0.450	-4.01

Table 7. Selection of descriptors at the HF/6-311G (d,p) level of approximation

Redox potential E			**Inhibitory concentration IC50**		
Equations	Linear correlation coefficient **IRI**	Descriptor rejected if **IRI < 0.50**	Equations	Linear correlation coefficient **IRI**	Descriptor rejected if **IRI < 0.50**
E and EHomo	0.03	Rejected	*LogIC50 and EHomo*	0.64	Withheld
E and $_{ELumo}$	0.43	Rejected	*LogIC50 and* $_{ELumo}$	0.56	Withheld
E and Gap	0.45	Rejected	*LogIC50 and Gap*	0.53	Withheld
E and χ	0.44	Rejected	*LogIC50 and* χ	0.66	Withheld
E and η	0.44	Rejected	*LogIC50 and* η	0.63	Withheld
E and S	0.41	Rejected	*LogIC50 and S*	0.64	Withheld
E and ω	0.44	Rejected	*LogIC50 and* ω	0.68	Withheld
E and μ	0.32	Rejected	*LogIC50 and* μ	0.52	Withheld
E and $\bar{\omega}^+$	0.42	Rejected	*LogIC50 and* $\bar{\omega}^+$	0.67	Withheld
E and $\bar{\omega}^-$	0.45	**Rejected**	*LogIC50 and* $\bar{\omega}^-$	0.68	**Withheld**

Table 8. Selection of descriptors at the AM1 level of approximation

Redox potential E			**Inhibitory concentration IC50**		
Equations	Linear correlation coefficient **IRI**	Descriptor rejected if **IRI < 0.50**	Equations	Linear correlation coefficient **IRI**	Descriptor rejected if **IRI < 0.50**
E and EHomo	0.61	Withheld	*LogIC50 and EHomo*	0.66	Withheld
E and $_{ELumo}$	0.81	Withheld	*LogIC50 and* $_{ELumo}$	0.66	Withheld
E and Gap	0.30	**Rejected**	*LogIC50 and Gap*	0.49	**Rejected**
E and χ	0.17	**Rejected**	*LogCI50 and* χ	0.18	**Rejected**
E and η	0.26	**Rejected**	*LogIC50 and* η	0.49	**Rejected**
E and S	0.29	**Rejected**	*LogIC50 and S*	0.31	**Rejected**
E and ω	0.42	**Rejected**	*LogIC50 and* ω	0.22	**Rejected**
E and μ	0.12	**Rejected**	*LogIC50 and* μ	0.10	**Rejected**
E and $\bar{\omega}^+$	0.61	Withheld	*LogIC50 and* $\bar{\omega}^+$	0.66	Withheld
E and $\bar{\omega}^-$	0.61	Withheld	*LogIC50 and* $\bar{\omega}^-$	0.66	Withheld

3.2 Selection of Quantum Descriptors for the Prediction of Redox Potential

The results for the final selection of the predictive quantum descriptors of the redox potential E are given in Tables 8 and 9.

The analysis of the results allows us to consider two groups of predictive quantum descriptors for the AM level1 :

- **Group 1**: LUMO energy ($_{ELumo}$), HOMO energy (*EHomo*) and electron donor power ($\bar{\omega}^-$**) ;**
- **Group 2:** Energy of the HOMO (*EHomo*), electron acceptor ($\bar{\omega}^+$) and electron donor power ($\bar{\omega}^-$**).**

For the HF/6-311G (d, p) method, no descriptor was retained, therefore there is no predictive model for redox potential at this level of calculation.

3.3 QSPR Model of the Predictive Quantum Descriptors of the Redox Potential *E* of the Inhibitory Concentration $LogIC_{50}$

Based on **the** learning **set** and the selected predictive descriptors, the aim were to :

- Establish one or more QSPR model(s) for predicting the redox potential *E* and the inhibitory concentration *LogIC50* per calculation level.
- to carry out an analysis of the statistical parameters of the QSPR models developed.

The results of this work allowed the validation of the best models for predicting the redox potential

E and the *LogIC50* inhibitory concentration of flavonoids.

3.3.1 QSPR model of predictive quantum descriptors of redox potential by the AM1 method

In order to select the group to be used for the regression equation of the QSPR model at the AM1 level of calculation, the Fisher coefficients of the two groups 1 and 2 compared and the most significant group in the Fisher sense selected.

Analysis of the results in Tables 10 and 11 shows that the Fisher coefficient ($_{F1}$) for Group 1 was higher than the Fisher coefficient (F2) for Group 2 : $\mathbf{F_2 < F_1}$ **;** this means that the regression equation for Group 1 will be more significant than that for Group 2. Therefore, the quantum descriptors of group 1 can be preferred to establish the QSPR model of the AM1 level of redox potential.

The ANOVA table for Model 1, which was used to perform the analysis of variance, is shown in Table 10. This ANOVA table indicates that the p-value (0.0005E-6) is less than α=0.05, showing that the regression equation of model 1 is significant in predicting redox potential.

The results of the multilinear regression obtained from the descriptors of group 1 are shown in Table 11.

The regression equation for model 1 is as follows :

$$E = -0.29 + 0.22E_{Homo} + 0.11E_{Lumo} - 0.05\bar{\omega}^{-}$$

3.3.2 Contribution of the AM1 level quantum descriptors in the prediction of the redox potential E

According to the absolute values of the t-test in Table 12, the importance of the quantum descriptors of the AM1 level in Model 1 is in the following order

$$\bar{\omega}^{-} < E_{Homo} < E_{Lumo}$$

Indeed, the contribution calculations show that the Lumo Energy ***(ELumo)*** makes a contribution of 48.35P in predicting the redox potential, the electron donor power ($\bar{\omega}^{-}$ **)** and the HOMO Energy (***EHomo***) make a contribution of 25.48P and 26.18P respectively. It is clear that the LUMO energy (***ELumo***) is the main predictive descriptor of the redox potential.

Table 9. ANOVA table of the quantum descriptors of group 1 of the AM1 level

	DS	SC	MSC	$_{F1}$	P-value
Regression	3	0.58	0.19	10.68	0.0005E-6
Residue	15	0.27	0.01		
Total	18	0.86			

Table 10. ANOVA table of the quantum descriptors of group 2 of the AM1 level

	DS	SC	MSC	F2	P-value
Regression	3	0.10	0.03	0.70	0.5634E-5
Residue	15	0.75	0.05		
Total	18	0.86			

Table 11. Values of the regression coefficients of group 1 for model 1

	Coefficients	Standard deviation	Test t	P-value
constants	-0.29	5.93	5.93	0.01
EHomo	0.22	0.02	0.02	0.20
ELumo	0.11	0.04	0.04	0.01
$\acute{\omega}^{-}$ ¿¿	-0.05	0.02	0.02	0.92

3.3.2 QSPR model of the predictive quantum descriptors of the *LogIC50* inhibitory concentration at the AM1 level: model 2

The ANOVA tables (Tables 12 and 13**)** show that the Fisher coefficient (F4) of group 3 is higher than the Fisher coefficient (F5) of group 4: $\mathbf{F_5 < F_4}$ **;** therefore, the quantum descriptors of group 4 can be preferred to establish the QSPR model of the AM1 level for the prediction of the inhibitory concentration.

The results of the multilinear regression obtained from the descriptors of group 4 are shown in Table 14.

The regression equation for model 2 is as follows:

$$LogIC_{50} = -4.92 + 11.37\ E_{Homo} + 34.36\ E_{Lumo} + 0.67\bar{\omega}^{-}$$

The ANOVA table for the model (Table 15) indicates that the p-value (0.00021E-7) is less than α = 0.05. Thus the regression equation of model 2 is significant in predicting the inhibitory concentration.

3.3.3 Contribution of AM1 quantum descriptors to the prediction of the inhibitory concentration

According to the absolute values of the t-test in Table 15, the importance of the quantum descriptors of the AM1 level in Model 2 was in the following order

$$\bar{\omega}^{-} < E_{Homo} < E_{Lumo}$$

The contribution calculations show that the Lumo Energy ($_{ELumo}$) makes a contribution of 60.66□ in predicting the redox potential, the electron donor power ($\bar{\omega}^{-}$) and the HOMO Energy (*EHomo*) make a contribution of 37.71□ and 2.25□ respectively. It is clear that the LUMO Energy ($_{ELumo}$) is the main descriptor predicting the inhibitory concentration.

3.3.4 QSPR model of the predictive quantum descriptors of the *LogIC50* inhibitory concentration at the HF/6-311G level (d, p): model 3

The Fisher coefficients for groups 5 and 6 are provided by the ANOVA tables in Tables 16 and 17. From the analysis of the results, the Fisher coefficient (F11) of group 5 is higher than the Fisher coefficients (F12) of group 6**;** its regression equation will be more significant than that of group 6.

The ANOVA table for Model 3 indicates that the p-value (p-value = 0.026E-8) is smaller than α=0.05. This shows that the regression equation of Model 3 is significant in predicting the inhibitory concentration of the molecules.

The results of the multilinear regression are shown in Table 17.

Table 12. ANOVA table of the quantum descriptors of group 3 of level AM1

	DS	SC	MSC	F4	P-value
Regression	3	2.84	3.96	4.33	0.00021E-7
Residue	15	3.87	3.59		
Total	18	6.71			

Table 13. ANOVA table of quantum descriptors for group 4 at AM1 level

	DS	SC	MSC	F5	P-value
Regression	3	3.65	7.82	1.16	0.00356E-4
Residue	15	4.06	8.20		
Total	18	5.71			

Table 14. Values of the regression coefficients of model 2 at AM1 level

	coefficients	Standard deviation	Test t	P-value
constants	-4.92	3.09	-3.36	0.00
EHomo	11.37	6.56	1.73	0.10
$\boldsymbol{E_{Lumo}}$	34.36	12.13	2.83	0.01
$\bar{\omega}^{-}$	0.67	6.38	0.10	0.91

The regression equation for model 6 is as follows:

$$LogIC_{50} = 62.40 + 80.25\ E_{Homo} - 28.44\ E_{lumo} + 52.01\ S - 71.26\ \eta - 6.11\mu$$

3.4 Statistical Parameters of Model 1 of Models 1, 2 and 3

The results of the statistical parameters are reported in Table 19.

The results show that :

- The redox potential is strongly correlated with the quantum descriptors of the AM1 level as R= 0.9820. In addition 96.43P of the experimental variance of the redox potential is explained by the descriptors of model 1. It can be said that model 1 is validated and can be retained as a model for predicting the redox potential of the studied molecules.
- The *LogIC50* inhibitory concentration is correlated with the quantum descriptors at the AM1 and HF/6-311G levels (d, p). Indeed, 96.35P and 99.96P of the experimental variance of the inhibitory concentration are explained by the descriptors of model 2 and model 3 respectively. It can be said that models 2 and 3 are validated and can be retained as a predictive model for the inhibitor concentration.

3.5 Internal LOO Validation of Models 1, 2 and 3

The results are reported in Table 20. They indicate that :

- Model 1 has a very high predictive capacity as 94.9P of the molecules in the training set have their redox potential predicted.
- Model 3 has a very high predictive ability, 98.9P of the molecules in the training set have their predicted inhibitory concentration.
- The model has a very high predictive capacity (Q^2_{Loo} = 0,941) because 94.1P of the molecules in the training set have their predicted inhibitory concentration

Table 15. ANOVA table of the quantum descriptors of group 5 of level HF/6-311G (d, p)

	DS	SC	MSC	F11	P-value
Regression	5	3.77	2.75	4.26	0.026E-8
Residue	13	3.16	2.55		
Total	18	6.93			

Table 16. ANOVA table of the quantum descriptors of group 6 of the HF/6-311G level (d, p)

	DS	SC	MSC	F12	P-value
Regression	5	6.65	1.32	0.83	0.546E-3
Residue	13	0.79	9.29		
Total	18	7.44			

Table 17. Values of the regression coefficients for group 5

	coefficients	Standard deviation	Test t	P-value
constants	62.40	63.74	0.05	0.95
EHomo	80.25	86.62	1.57	0.13
Elumo	-28.44	16.71	-2.35	0.03
S	52.01	40.83	0.36	0.72
η	-71.26	24.56	-0.13	0.89
μ	-6.11	7.58	-0.80	0.43

Table 18. Statistical parameters for the external validation of models 1, 2 and 3

Models	*n*	*R*	*R2*	*Rzaj*	*S*	*F*	*FIT*
Model1	19	0.9820	0.9643	0.9582	0.0755	4.3492	0.230
Model2		0.9816	0.9635	0.8575	0.0850	4.3397	0.023
Model 3		0,998	0,996	0,8936	0,2498	4,2614	0.080

3.6 External Validation of Models 1, 2 and 3

The results are reported in Table 20 and show that :

- Model 1, has high predictive power (Q2ext = 0.891) as 89, 1.P of the molecules in the test series have their redox potential predicted. In addition 93, 50% of the experimental variance in redox potential is explained by the quantum descriptors of model1 at the AM1 level.
- Model 2, has a high predictive power. Indeed, 97.80P of the molecules in the test series have their redox potential predicted. In addition 98.30% of the experimental variance of the inhibitory concentration is explained by the quantum descriptors of model 2 at the AM1 level.
- Model 3 has high predictive power as 96.10P of the molecules in the test series have their redox potential predicted. Also, 97.70P of the experimental variance in the percentage of inhibition is explained by the quantum descriptors of model 3 at the HF/6-311G level (d, p).

3.7 Verification of Tropsha Criteria for Models 1, 2 and 3

The analysis of the results is recorded in Table 21 and shows that :

- For model 1 only criteria 1, 2 and 4 are verified; i.e. the of Tropsha's criteria. The model is therefore efficient in predicting the redox potential
- For model 2, only criteria 1, 2 and 4 are verified while for model 3, all 5 criteria are verified. Models 2 and 3 therefore perform very well in predicting the inhibitory concentration.

3.8 Normality Tests of Models

3.8.1 Normality tests for model 1

- **Shapiro-Wilk test (*Epréd*)**

This test gives the following results: w = 0.390; p-value = 0.879; α =0.05

Table 19. Statistical parameters for internal and external validation of models 1, 2 and 3

Model 1	**Internal**	***n***	***PRESS***	Q^2_{Loo}	S_{Press}	
		19	0.197	0.949	0.170	
	Extern	***n***	R^2_{ext}	***PRESS***	***Q²ext***	S_{PRESS}
		10	0.935	0.149	0.891	0.044
Model 2	**Internal**	***n***	***PRESS***	Q^2_{Loo}	S_{Press}	
		19	0.221	0.989	0.134	
	Extern	***n***	R^2_{ext}	***PRESS***	***Q²ext***	S_{PRESS}
		10	0.983	0.149	0.978	0.116
Model 3	**Internal**	***n***	***PRESS***	Q^2_{Loo}	S_{Press}	
		19	0.256	0.941	0.322	
	Extern	***n***	R^2_{ext}	***PRESS***	***Q²ext***	S_{PRESS}
		10	0.977	0.198	0.961	0.143

Table 20. Tropsha criteria verification for the models developed [15] (T. M. Martin et al.; 2012)

Criteria	**Model 1**	**Model2**	**Model 3**
Critrion 1 = $R^2_{ext} > 0.70 > 0.70$	0.935	0.953	0.877
Critrion 2 = *Q²ext* > 0.60	0.891	0.918	0.853
Critrion 3 = $\frac{R^2_{ext}-R^2_0}{R^2_{ext}}$ **< 0.1 et 0.85 < *k* < 1.15**	0.010	0.058	0.139
Critrion 4 = $\frac{R^2_{ext}-R'^2_0}{R^2_{ext}}$ **< 0.1 et 0.85 < *k'* < 1.15**	0.011	0.041	1.528
Critrion 5= $\lvert R^2_{ext} - R^2_0 \rvert \leq 0.30$	0.03	0.023	0.121

Interpretation of the test: Since the calculated p-value is above the alpha threshold significance level (0.879 > 0.05), it is concluded that the predicted values of the redox potential by model 1 follow a normal distribution.

- **Durbin-Watson test (residuals) :**

This test gives the following results: U= 0.785; p-value = 0.4860; α = 0.05

Interpretation of the test: Since the calculated p-value is above the alpha significance level (0.4860 > 0.05), it is concluded that the residuals are not autocorrelated. Therefore, they do not contain any information that could influence the prediction of model 1.

3.8.2 Normality tests of model 2

- **Shapiro-Wilk test**

This test gives the following results: w = 0.239; p-value = 0.067; α =0.05

Interpretation of the test: Since the calculated p-value is above the alpha threshold significance level (0.067 > 0.05), it is concluded that the predicted values of the inhibitory concentration by model 2 follow a normal distribution.

- **Durbin-Watson test:**

This test gives the following results: U=0.463; p-value = 0.1137; α =0.05

Interpretation of the test: Since the calculated p-value is above the alpha significance level, the residuals are not autocorrelated. They do not contain any information that could influence the prediction of model 2.

3.8.3 Normality tests of model 3

The results are as follows:

- **Shapiro-Wilk test**

This test gives the following results: w=0.105; p-value = 0.077; α =0.05

Interpretation of the test: Since the calculated p-value is above the alpha threshold significance level (0.077 > 0.05), it is concluded that the predicted values of their inhibitory concentration by model 3 follow a normal distribution.

- **Durbin-Watson test:**

This test gives the following results: U=0.993; p-value = 0.1232; α =0.05

Interpretation of the test: Since the calculated p-value is above the alpha significance level, the residuals do not contain information that could influence the prediction of model 3.

3.8.4 Predicted model equations

From the various statistical tests in Table 18 we can deduce that the equations of the models are as follows:

Model 1: Prediction of the redox potential, which is summarized as follows:

$$E = -0.29 + 0.22E_{Homo} + 0.11ELumo - 0.05\bar{\omega}^{-}$$

***n*=**19; R**=**0.9820 ; $\mathbf{R^2}$ **=**0.643 ; $\boldsymbol{R^2_{aj}}$ **=** 0.9582 ; ***S* =** 0.0755 ; ***F*=**4.3492 ; ***FIT*=**0.230

Model 2: Prediction of the inhibitory concentration is summarised as follows at the AM1 level:

$$LogIC_{50} = -4.92 + 11.37E_{Homo} + 34.36\ E_{Lumo} + 0.67\bar{\omega}^{-}$$

***n*=**19; ***R* =** 0.9816*;* $\boldsymbol{R^2}$ **=** 0.9635; $\boldsymbol{R^2_{aj}}$ **=** 0.8575; ***S*=**0.0850; ***F*=**4.3492 ; ***FIT* =** 0.0230

Model 3: The prediction regression equation is summarised as follows:

$$LogIC_{50} = 62.40 + 80.25\ E_{Homo} - 28.44\ E_{lumo} + 52.01\ S - 712.6\ \eta - 6.11\mu$$

***n*=**19; ***R* =**0.998; $\mathbf{R^2}$ **=**0.998; $\boldsymbol{R^2_{aj}}$ **=** 0.996; ***S*=** 0.24936; ***F*=**1.4614; ***FIT*=**0.08

3.9 Predicted Values of Redox Potential and Inhibitory Concentration of 29 Flavonoids by Models 1, 2, 3

Table 21 shows the predicted values of redox potential and percentage inhibition of the 29 flavonoids by models 1, 2 and 3.

These results show that there is good agreement between the model values and the experimental values published in the literature.

Table 21. Experimental and predicted values of redox potential and inhibitory concentration of the 29 flavonoids by the models

Code	*E*		*LogIC50*		
	Exp	**Mod1**	**Exp**	**Mod 2**	**Mod3**
M1	-0.035	-0.038	-4.80	-4.84	-4.87
M2	-0.020	-0.021	-4.96	-4.95	-4.91
M3	-0.010	-0.008	-4.89	-4.91	-4.85
M4	0.040	0.038	-4.89	-4.91	-4.85
M5	0.080	0.076	-5.00	-4.97	-4.95
M6	0.082	0.086	-4.60	-4.66	-4.68
M7	0.082	0.086	-4.52	-4.53	-4.49
M8	0.092	0.097	-4.42	-4.39	-4.37
M9	0.102	0.107	-4.29	-4.27	-4.25
M10	0.450	0.453	-4.01	-3.98	-3.94
M11	0.180	0.177	-4.58	-4.57	-4.54
M12	0.360	0.356	-	-	-
M13	0.500	0.496	-	-	-
M14	0.132	0.134	4.18	4.15	4.13
M15	0.590	0.591	-	-	-
M16	0.500	0.503	-	-	-
M17	0.538	0.537	-	-	-
M18	0.540	0.542	-	-	-
M19	-0.030	-0.028	-4.53	-4.51	-4.49
M20	-0.030	-0.032	-4.98	-4.95	-4.94
M21	0.020	0.023	-5.07	-5.02	-5.03
M22	0.030	0.027	-4.68	-4.65	-4.62
M23	0.080	0.084	-4.72	-4.76	-4.73
M24	0.105	0.101	-4.64	-4.65	-4.62
M25	0.280	0.279	-4.86	-4.78	-4.74
F26	0.180	0.177	-4.03	-3.97	-3.95
M27	0.185	0.183	-4.23	-4.21	-4.18
M28	-0.060	-0.059	-5.20	-5.21	-5.25
M29	0.080	0.076	-4.70	-4.67	-4.65

4. CONCLUSION

A prediction study of the redox potential *E* and the inhibitory concentration *LogIC50* was performed, using the semi-empirical methods AM1 and HF/6-311G (d, p).

- ✓ The application of the descriptor selection criteria made it possible to determine and retain 6 groups of quantum descriptors, including 2 groups of descriptors for the prediction of the redox potential *E* and 4 groups of descriptors for the prediction of the inhibitory concentration *LogIC50*. The antioxidant properties of the molecules depend strongly on these groups of descriptors.
- ✓ From the multilinear regression analysis, several prediction models (one model for redox potential and two for inhibitory concentration) were established from the quantum descriptors. The established models are validated and perform well according to Tropsha criteria.

The development of these QSPR models represents a significant advance in the prediction of antioxidant properties of bioactive molecules such as flavonoids based on descriptors calculated by quantum chemical methods. This is a contribution to the database of the two main parameters (E and IC50) involved in the prediction of antioxidant properties of bioactive molecules.

COMPETING INTERESTS

Authors have declared that no competing interests exist.

REFERENCES

1. Hendrickson HP, Kaufman AD, Lunte CE. J. Pharm. Biomed Anal. 1994;12:325.

2. Jovanovic SV, Steenken S, Simic MG, Hara Y. Antioxidant properties of flavonoids: Reduction potentials and electron, transfer reductions of flavonoid radicals. In: Rice-Evans, C. A.; Packers, L., eds. Flavonoids in health and disease. New York: Marcel Dekker, Inc. 1996;137-161.
3. Labuda J, Buková M, Heilerová L, Šilhár S, Štepánek I. Evaluation of the redox properties and anti/pro-oxidant effects of selected flavonoids by means of a DNA-based electrochemical biosensor. Anal Bioanal Chem. 2003;376:168-173.
4. José T, Alexandra G, Manuela E, Garrido JG, Fernanda B. Hydroxycinnamic acid antioxidants: An electrochemical overview, hindawi publishing corporation bio med research international. Article ID 251754. 2013;11.
5. Lien EJ, Ren S, Bui HH, Wang R. Free Radic. Biol. Med. 1999;26:285.
6. Bin Y, Akira K, Kensunke A, Fumiyo K. Estimation of the antioxidant activities of flavonoids from their oxidation potentials. Analytical sciences; the Japan society for analytical chemistry. 2001;1.
7. Pearson RG. Hard and soft acids and bases, J. Am. Chem. Soc. 85, 3533-3539, (1963),(2001).
8. R. G. Parr, R. A. Donnelly, M. Levy, W. E. Palke. J. Chem. Phys. 1978;68:3801-3807.
9. Geerlings P, De Proft F, Langenaeker W. Chem. Rev, 2003 ;103 :1793-1874.
10. Caro A, Zagal JH, Bedioui F, Adamo C, Cardenas-Jiron GI. J. Phys. Chem. A. 2004;108:6045-6051.
11. De Vleeschouwer F, Jaque P, Geerlings P, Toro-Labbe A, De Proft F. J. Org Chem. 2010;75:4964-4974.
12. Morrel H Cohen, Adam W. Journal of Statistical Physics, On Hardness and Electronegativity Equalization in Chemical Reactivity Theory; 2006.
13. Bonin KD. Kresin electric-dipole polarizabilities of atoms molecules and clusters. World Scientific, Singapore, VV; 1997.
14. Payán G, Sergio A, Norma Flores H, Antonino P, Manuel Piñón M, Daniel G. Computational molecular characterization of the flavonoid rutin. Chemistry Central Journal. 2010;4:12.
15. Laffly. Multiple regression: principles and application examples; 2006.
16. Golbraikh A. Tropsha, beware of q2 J. Mol. Graph. Model. 2002;20:269-276.
17. Dragan A, Duanka D, Drago B, Vesna R, Bono L, Nenad T. SAR and QSAR of the antioxidant activity of flavonoids. Current Medicinal Chemistry. 2007;14:827-845.
18. Durbin J, Watson GS. Testing for serial correlation in least squares regression II. Biometrika. 1951;38(1-2):159-179.
19. Tetko V, Sushko I, Pandey AK, Zhu H, Tropsha A, Papa E, Oberg T, Todeschini R, Fourches D, Varnek A. J. Chem. Inf. Model. 2008;48:1733.
20. Jovanovic SV, Steenken S, Hara Y, Simic MG. Reduction potentials of flavonoid and model phenoxyl radicals which ring in flavonoids is responsible for antioxidant New York: Marcel Dekker, Inc. 1998;137-161.
21. Jaworska J, Jeliazkova NN, Aldenberg T. Altern. Lab. Anim. 2005;33:445-459.
22. Jorgensen LV, Cornett C, Justesen U, Skibsted LH, Dragsted LO. Free Rad. Res. 1998;29:339.
23. Medjdoub GA. Contribution to the study of chemical reactivity using conceptual DFT, application to heterocycle chemistry; 2012.
24. Chattaraj PK, Perez P, Zevallos J, Toro-Labbe A. J. Phys. Chem. A. 2006 ;104 :4272-4283.
25. Rubalya V, S, Neelamegam P. Selective ABTS and DPPH- radical scavenging activity of peroxide from vegetable oils , International Food Research Journal. Journal homepage. 2015;22(1):289-294.
26. Shapiro SS, Wilk MB. An analysis of variance test for normality (Complete Samples). Biometrika. 1965;52(3 and 4):591-611.

Peer-review history:
The peer review history for this paper can be accessed here:
https://www.sdiarticle4.com/review-history/72000

ISSN Print: 2664-6552
ISSN Online: 2664-6560
Impact Factor: RJIF 5.5
IJCRD 2023; 5(1): 09-17
https://www.chemicaljournal.in/
Received: 15-11-2022
Accepted: 20-12-2022

R Chabi Doco
Laboratory of Theoretical Chemistry and Molecular Spectroscopy (LACTHESMO), University of Abomey-Calavi, 03 BP 3409 Cotonou-Benin

MTA Kpota Houngue
Laboratory of Theoretical Chemistry and Molecular Spectroscopy (LACTHESMO), University of Abomey-Calavi, 03 BP 3409 Cotonou-Benin

Urbain A Kuevi
Laboratory of Theoretical Chemistry and Molecular Spectroscopy (LACTHESMO), University of Abomey-Calavi, 03 BP 3409 Cotonou-Benin

YGS Atohoun
Laboratory of Theoretical Chemistry and Molecular Spectroscopy (LACTHESMO), University of Abomey-Calavi, 03 BP 3409 Cotonou-Benin

Corresponding Author:
R Chabi Doco
Laboratory of Theoretical Chemistry and Molecular Spectroscopy (LACTHESMO), University of Abomey-Calavi, 03 BP 3409 Cotonou-Benin

Theoretical study of the reactivity of urea, thiourea and some of their hydroxylated derivatives towards free radicals

R Chabi Doco, MTA Kpota Houngue, Urbain A Kuevi and YGS Atohoun

DOI: https://doi.org/10.33545/26646552.2023.v5.i1a.43

Abstract
Urea is an organic compound with the chemical formula $CO(NH_2)_2$. It is similar to thiourea of formula $CS(NH_2)_2$, except that the oxygen atom is replaced by a sulfur atom. It has been shown that urea and thiourea, have derivatives such as: Enolurea, hydroxyurea, hydroxyhiourea, enolthiourea.

Indeed, since the discovery of these different compounds, the results of *in vitro* tests have shown the capacity of each of them to participate in the antioxidant defence of the body by trapping free radicals.

In the present work, a comparative study of the antioxidant properties of urea, enolurea, thiourea, 1-hydroxyurea, hydroxythiourea and enolthiourea was carried out by DFT method M06-2X/6-311++G (d, p).

The results of the various calculations allowed to:

- Identify the oxygen atoms of the O-H groups, O-H^9, O-H^7 and O-H^8, as the most important sites for the manifestation of the antioxidant activity of hydroxythiourea, hydroxyurea, enolthiourea and Enolurea respectively.
- It was found that thiourea and hydroxythiourea are the most antioxidant of the six molecules.
- to note that the replacement of the oxygen atom by that of sulfur considerably modifies the antioxidant properties of the urea molecule to note that the mechanism passing by the elimination of atomic hydrogen by homolytic rupture of bond (HAT), as the most probable for the trapping of a radical by each of the molecules.

Keywords: DFT, antioxidant, urea, thiourea

Introduction

Urea is an organic compound with the chemical formula $CO(NH_2)_2$. It is a small polar molecule with three resonance structures. It is generally synthesized in the liver and then transported by the blood to the kidneys. Experimental work published in the literature has shown that urea is also obtained by conversion of ammonia [1].

The kinetics of urea production, excretion and hydrolysis have been extensively studied in humans [2]. However, very little research has been devoted to the roles of urea in the body [3]. Traditionally, urea has played a passive role in the body. One of its functions is related to the fact that it is an osmotically active substance. Thus, changes in its concentration can contribute to osmoregulation in the kidneys [4]. Other studies have shown that it also stimulates transcription and expression of immediate early genes [5]. It is used in many fields, such as agricultural, pharmaceutical, chemical and medical industries [6].

On the experimental level, the capacity of urea to trap radical species has been reported in the literature. Indeed, the results of *in vitro* tests have shown the capacity of urea to trap free radicals, thus proving its participation in the antioxidant defence of the body. Moreover, an increase in the antioxidant capacity of serum has been observed in patients suffering from kidney disease. This increase would be entirely due to the relatively high serum urea present in the patients examined. In contrast, after hemodialysis when the serum urea concentration was significantly decreased, the antioxidant capacity of serum was significantly reduced [7]. Some works have also shown that due to its low molecular weight, urea seems to be more mobile compared to macromolecular antioxidants such as superoxide dismutase (SOD), catalase (CAT) and ceruloplasmin (CP), whose total antioxidant capacity seems to be confined by their limited mobility and for some, their compartmentalized distribution [8].

On the theoretical level, several works published in the literature have shown that urea has antioxidant properties, for example, by DFT / BHHLYP and DFT/ωB97X-D methods, it was shown that the direct H-atom abstraction mechanism is kinetically preferred to the OH radical addition reaction [9]. In the same year, a M06-2X/6-311++G (d, p) study found that the superoxide radical anion can effectively abstract a hydrogen atom from one of the amino groups of urea and thiourea in aqueous media. They therefore concluded that these two compounds would both serve as very efficient scavengers of superoxide radical anion [10].

In addition, it has been shown experimentally in the literature, that urea has derivatives such as: Enolurea, thiourea, hydroxyurea, hydroxythiourea and enolthiourea. The latter are recognized as antioxidants due to their ability to trap radical species and reduce hydrogen peroxide. They are involved in the protection of cardiac rhythm and coronary flow [11].

Thiourea is a sulfur derivative of urea with the formula $CH_4 N_2 S$. It is similar to urea, except that the oxygen atom is replaced by a sulfur atom. They present all of them, two (02) tautomeric forms. The properties of urea and thiourea differ considerably due to the relative electronegativities of sulfur and oxygen [12]. Various experimental studies published in the literature have shown that thiourea has antiviral [13] and antifungal properties [14]. Hydroxyurea ($CH_4 N_2 0_2$) differs from urea by the presence of a hydroxyl group on one of the nitrogen atoms [15]. This molecule is recognized as a non-alkylating antineoplastic and antiviral agent used in hematology, oncology, infectious diseases and dermatology [16].

From all the above, it should be noted that to our knowledge, no theoretical or experimental work has compared the antioxidant powers of urea, enolurea, thiourea, hydroxyurea and hydroxythiourea. The objective of the present work is to determine the best antioxidant among these compounds by the methods of theoretical chemistry. The reactivities of the different compounds will be compared between them, in order to deduce the most antioxidant of these molecules.

To achieve this objective, different electronic and spectroscopic parameters will be calculated and the results will allow to deduce a ranking order of the antioxidant powers of each compound.

Materials

The chemical systems object of our study were: urea, enolurea, thiourea, hydroxyurea, hydroxythiourea and enolthiourea

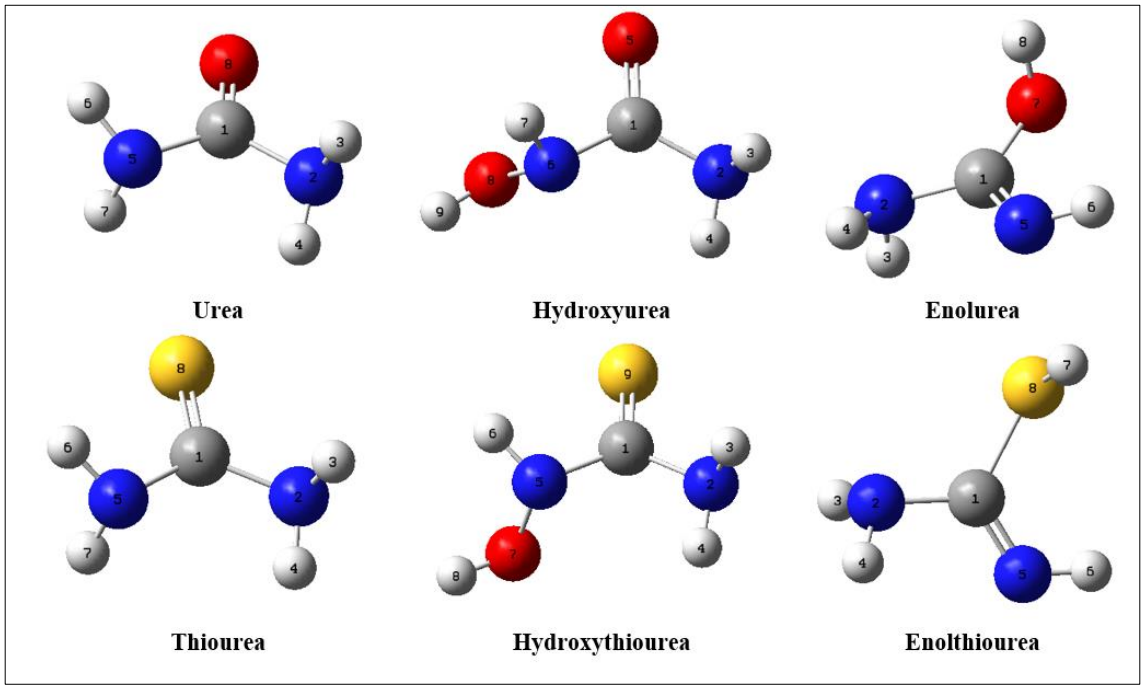

Fig 1: Optimized form of each compound

Methodology

For urea, Enolurea, thiourea, hydroxyurea, hydroxythiourea and enolthiourea, the calculated parameters were:

- **Electronic parameters**
- The Energy *Gap* $_{(HOMO\text{-}LUMO)} = E_{LUMO} - E_{HOMO}$ which is all the lower that the molecule has a high antioxidant power
- The electronic affinity (*AE*): $AE=-E_{LUMO}$; the ionization energy $EI = -E_{HOMO}$ [17].
- The dipole moment (*M*) which accounts for the greater or lesser polarity of a molecule
- The hardness (η) which expresses the resistance of a molecule to the change of its electron number or charge transfer [18]. The stronger the hardness, the less reactive the molecule: $\eta = \frac{(ELUMO - EHOMO)}{2}$
- The electronegativity (χ) which measures the tendency of a chemical species to attract electrons [18]: $\chi = \frac{-(ELUMO + EHOMO)}{2}$
- The electrophilic index (ω) which is the stabilization energy of a molecule saturated by electrons from its surroundings [18]: $\omega = \frac{\chi^2}{2\eta}$
- The redox potential E^0 of the molecules, given by the relation of Nerst.

$E^0 = \frac{-\Delta G^o}{nF}$

With ΔG^o the Gibbs energy related to the reaction $Ox \rightarrow +nH_{❑}^{++ne}$ n the number of transferred electron and F the Faraday constant.

The lower the redox potential of a molecule, the higher its antioxidant activity [19]. Since the redox potential is measured in the aqueous phase, the calculation of ΔG^o requires the use of the Born-Haber cycle.

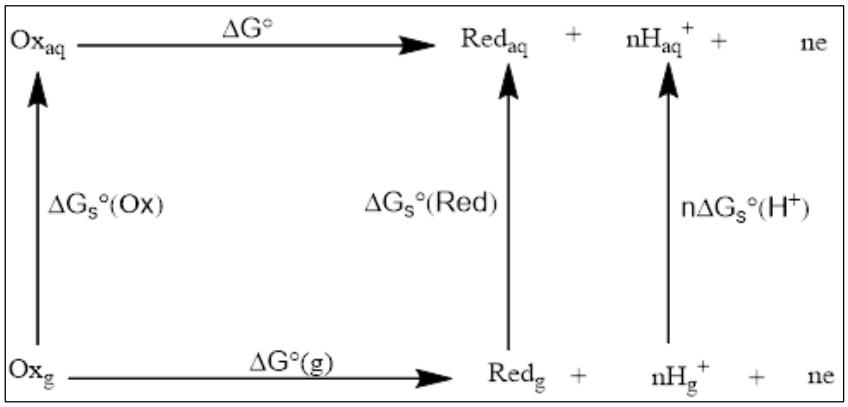

Scheme 1: Born-Haber cycle for obtaining ΔG^0 from $\Delta G°(g)$

$\Delta G_s^o(H+) = -1104.6\ kJ.mol^{-1}$

On the basis of this cycle we can establish:

$\Delta G^0 = \Delta G_s^\circ + \Delta G^\circ(g) + n\,\Delta G_s^\circ(H^+) - \Delta G_s^\circ(Ox)$

- Spectroscopic parameters such as infrared and UV-visible spectra were calculated by the TD-DFT method. These parameters will allow on the one hand to find the influence of antioxidant properties on the variation of the chemical function and on the other hand to compare the antioxidant properties of the compounds.
- Studies of the mechanisms of antioxidant activity of molecules in the present work, it was considered to determine the most probable routes of the reactions that take place between the studied molecules. For this purpose, three different types of ways of manifestation of the antiradical activity of the molecules have been examined.
  - The elimination of an electron ($ArOH \rightarrow ArOH^{\circ+}+e^-$), followed by that of a proton), (Single-Electron Transfer - Proton Transfer (SET-PT)). For this purpose, the formula: SETPT = $\Delta H(ArO^\bullet)$ ΔH) - ΔH)
  - The elimination of a proton ($ArOH \rightarrow ArO^{-}+H^+$), followed by that of an electron), (Sequential Proton Loss Electron Transfer (SPLET)); then trapping of free radicals. For this purpose the affinity formula :

SPLET = $\Delta H(ArO^\bullet)$ + ΔH**)** + $\Delta H(e)$ - $\Delta H(ArOH^{❑})$

The elimination of a hydrogen atom by homolytic OH) and then trapping of free radicals. For this purpose the BDE (Bond Dissociation Energy) has been calculated:

$BDE = \Delta H(ArO^\bullet) + \Delta H(H^\cdot) - \Delta H(ArOH^{❑})$

For each of these three reaction paths, an energy balance has been made. The lower the total energy released on a reaction pathway, the more likely this pathway will be. On the basis of such an energy balance, we can then propose the most probable mechanism of manifestation of the antiradical activity of the studied molecules, and determine the hydroxyl sites most favorable to this manifestation.

H(ArOH): Enthalpy of the ArOH molecule; H (ArO•): Enthalpy of the ArO radical**•;**
H (ArOH• +): Enthalpy of the cation radical $ArOH^{\circ+}$H (ArO-): Enthalpy of the anion ArO^{-}**;**
H(e-): Enthalpy of the electron (0.752 Kcal/mol) [20];
H (H+): Enthalpy of the proton (1.482 Kcal/mol) [20];

Representation of molecular electrostatic potentials in three dimensions (3D)

The electrostatic potential gives information about the nuclear and electronic charge distribution of molecules. It is an indispensable tool for the interpretation and prediction of chemical reactivity. It is widely used as a molecular reactivity map because it displays the most probable regions for nucleophilic and electrophilic attacks. Indeed, in the potential energy surface, the red color refers to an electron-rich (negative) region, the blue color refers to an electron-poor (positive) region and the green color means a zero electrostatic potential. In most surface energy surfaces, the negative region is the preferred site for electrophilic attack and the positive region is preferred for nucleophilic attack [22].

Results and Discussions

Analysis of the electronic parameters of urea, Enolurea, thiourea, hydroxyurea, hydroxythiourea and enolthiourea

The calculated values of the electronic parameters, at the M06-2X approximation level of each of the six molecules are recorded in the following Table 1:

Table 1: Calculated values (kJ/mol) of *the* electronic parameters of urea, enolurea, thiourea, hydroxyurea, hydroxythiourea and enolthiourea

	E_{Gap}	AE	EI	μ	ω	η	χ
Urea	204.54	8.15	212.72	3.79	59.62	102.27	110.43
Enolurea	193.9	8.78	202.68	3.01	57.65	96.95	105.73
Hydroxyurea	203.94	8.15	212.09	3.94	59.49	101.97	110.12
Thiourea	156.87	11.92	168.79	5.07	52.04	78.43	90.35
Enolthour	191.39	5.64	197.03	2.28	53.65	95.69	101.33
Hydroxythiourea	161.27	11.92	173.19	4.61	53.11	80.63	92.55

The results in Table 1 show that:

The six molecules, thiourea gave the lowest Gap value (HOMO-LUMO) followed by hydroxythiourea. This result in agreement with experimental data published in the literature, means that thiourea and hydroxythiourea are much less stable and therefore more antioxidant than urea, enolurea, hydroxyurea and enolthiourea [23].

Overall, the Gaps ranking order of the six molecules would be: thiourea < hydroxythiourea < enolthiourea < hydroxyurea < urea by decreasing order of the antioxidant activity; we have thus thiourea - hydroxythiourea - enolthiourea - hydroxyurea - urea. The thiourea would be the most antioxidant of the six molecules.

- The six compounds, the lowest values of hardness (η), electronegativity (χ) and electrophilic index (ω) on the one hand, the highest value of dipole moment (μ) on the other hand were obtained respectively by thiourea and hydroxythiourea. These series of results show more that thiourea followed by hydroxythiourea are the most antioxidant of the molecules. Also, the values obtained of the dipole moment reveal that thiourea and hydroxythiourea are more polar than enolthiourea, hydroxyurea and urea.
- It appears from these analyses that thiourea and hydroxythiourea are more antioxidant than enolthiourea, Enolurea, hydroxyurea and urea.

Calculation of the redox potentials of molecules

The redox potentials (**E°)** of the six molecules, calculated by the M06-2X functional method in bases 6-311++G (d, p) are reported in Table 2.

Table 2: Calculated values (in volt) of the redox potential *of* urea, enolurea, thiourea, hydroxyurea, hydroxythiourea and enolthiourea

	M06-2X / 6-311++G (d,p)
Urea	-0.47
Enolurea	-0.61
Hydroxyurea	-0.49
Thiourea	-0.83
Enolthour	-0.67
Hydroxythiourea	-0.75

From the analysis of the results in Table 2, it appears that the lowest values of redox potentials obtained in the order: Thiourea < hydroxythiourea < enolthiourea < hydroxyurea < urea.

This result further indicates that thiourea followed by hydroxythiourea are the most antioxidant of the six (06).

Determination of the probable hydroxyl sites of antioxidant activity of the molecules

For the different O-H bonds found in urea, Enolurea, thiourea, hydroxyurea, hydroxythiourea and enolthiourea molecules, the values of the bond breaking enthalpies (BDE) were calculated at the M06-2X approximation levels. The results obtained are reported in Table 3.

Table 3: Values (in kcal/mol) of O-H bond breaking enthalpies (BDE) calculated at the M06-2X approximation levels for urea, enolurea, thiourea, hydroxyurea, hydroxythiourea and enolthiourea

Links		**M06-2X/6-311++G (d,p)**
Urea	O-H[4]	116.08
	O-H[6]	109.18
Enolurea	O-H[4]	106.675
	O-H[8]	97.26
Thiourea	O-H[4]	46.43
	O-H[9]	84.71
Hydroxyurea	O-H[7]	90.98
	O-H[4]	116.71
	O-H[8]	79.06
Hydroxythiourea	O-H[6]	94.75
	O-H[4]	109.185
	O-H[6]	104.16
Enolthiourea	O-H[4]	109.81
	O-H[7]	89.105

The results in Table 3 show that:

- Of the six molecules, the lowest values of dissociation enthalpy by homolytic OH bond breaking (BDE) was obtained by thiourea. This result further confirms that thiourea is the most antioxidant of the six molecules.
- For hydroxythiourea, hydroxyurea, enolthiourea and Enolurea, the lowest enthalpy values are mainly obtained for the bonds

O-H[8], O-H[9], O-H[7] and O-H[8] respectively. These results indicate that the hydrogen atoms H[8], H[9], H[7] and H[8] can easily dissociate from each of the four molecules to release radicals that can scavenge free radicals. Thus, the O-H[8], O-H[9], O-H[7] and O-H[8] sites appear to be the most important for the manifestation of antioxidant activity of hydroxythiourea, hydroxyurea, enolthiourea and Enolurea respectively.

- Overall, the BDE values given for each of the molecules are ranked in order: Thiourea < hydroxythiourea < enolthiourea < hydroxyurea < Enolurea < urea.

The antioxidant activity of thiourea would thus be more important than that of the other six molecules

Mechanisms and sites of manifestation of antiradical activity of molecules

For the different O-H bonds found in each of the molecules, the calculated values of the different energy parameters (HAT SETPT and SPLET), relative to the three reaction paths considered, are recorded in Table 5.

Table 5: Calculated values (in kcal/mol) of the energy parameters of urea, Enolurea, thiourea, hydroxyurea, hydroxythiourea and enolthiourea

	Urea	Enolurea	Thiourea	Enolthiourea	Hydroxyurea	Hydroxythiourea
HAT	116.08	97.26	46.43	89.105	84.71	79.06
SETPT	430.06	411.23	360.41	403.08	404.96	393.04
SPLET	430.81	411.98	361.16	403.83	405.71	393.79

The results obtained for urea, Enolurea, thiourea, hydroxyurea, hydroxythiourea and enolthiourea show that the reaction pathway passing through the elimination of a hydrogen atom by homolytic rupture of the O-H bond required the lowest energy values. This means that the manifestation of the antiradical activity of each of the six molecules, would probably pass by this last reaction path (elimination of a hydrogen atom by homolytic rupture of OH bond then scavenging of the free radicals).

Study of the uv-visible spectra of urea, Enolurea, thiourea, hydroxyurea, hydroxythiourea and enolthiourea

The absorption curves of the UV-Visible spectrum of each of the six molecules were calculated and represented at the level M06-2X/6-311++G (d, p) (Figure 2).

From the analysis of the different absorption curves it appears that:

- Urea, Enolurea and hydroxyurea have respectively 3, 5, 2 peaks of UV-vis absorption whose band width varies between 50 nm and 230 nm. Regarding thiourea, hydroxythiourea and enolthiourea they present 8, 7 and 4 peaks respectively whose absorption band is between 300 nm and 350 nm. It follows from these results that thiourea, hydroxythiourea and enolthiourea appear more antioxidant than urea, Enolurea and hydroxyurea. These last molecules having presented a range of absorption band less broad than thiourea, hydroxythiourea and enolthiourea. Indeed, according to the experimental work published in the literature by [24], the molecules presenting a broad range of UV-vis spectra facilitate more the electronic delocalization and present a strong antioxidant character.
- The comparison between the UV-visible absorption spectra of urea, Enolurea, thiourea, hydroxyurea, hydroxythiourea and enolthiourea showed that thiourea and hydroxythiourea had the widest absorption bands. This means that thiourea and hydroxythiourea have the strongest antioxidant powers of the six molecules.

From all the above, it should be said that thiourea and hydroxythiourea are antioxidant than urea, enolurea, hydroxyurea and enolthiourea.

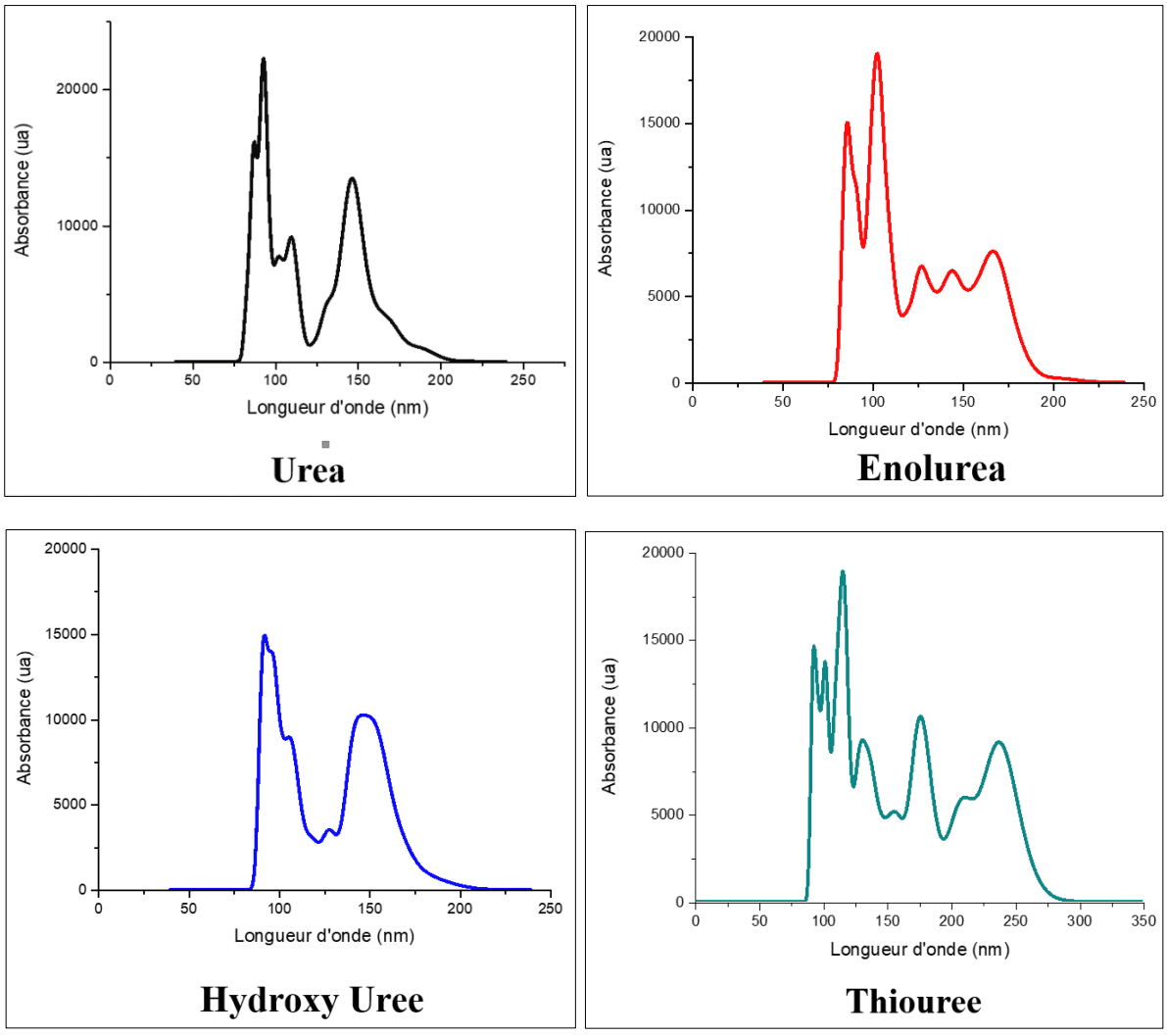

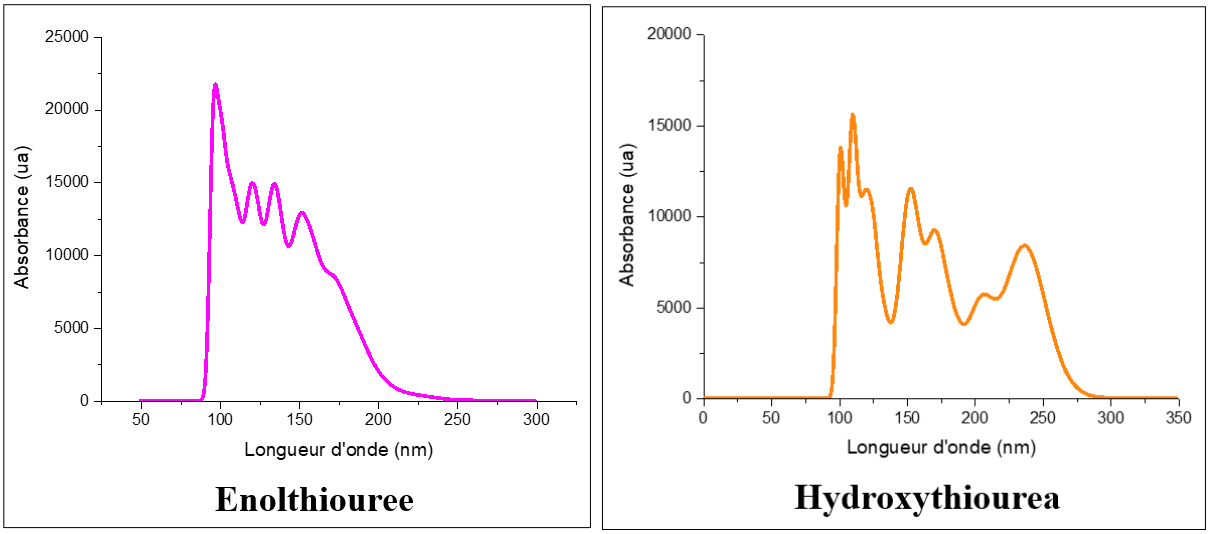

Fig 2: Uv-visible spectra of urea, Enolurea, thiourea, hydroxyurea, hydroxythiourea and enolthiourea

Analysis of the Infra-Red spectra of urea, Enolurea, thiourea, hydroxyurea, hydroxythiourea and enolthiourea

The IR spectra of urea, Enolurea, thiourea, hydroxyurea, hydroxythiourea and enolthiourea are shown in Figure 3.

From the analysis of the different spectra, it appears that:

- Infrared spectra of urea, Enolurea and hydroxyurea are dominated by intense bands located in the spectral range 0 to 2000 cm^{-1}. For thiourea, hydroxythiourea and enolthiourea less intense IR spectral bands between 0 cm^{-1} and 1800 cm^{-1} were observed. From these observations, it appears that thiourea, hydroxythiourea and enolthiourea appear to be more stable than urea, Enolurea and hydroxyurea
- IR spectra of urea, Enolurea and hydroxyurea gave much less intense bands than those of thiourea, hydroxythiourea and enolthiourea. This result indicates that electron delocalization would be more important in urea, Enolurea and hydroxyurea than in thiourea, hydroxythiourea and enolthiourea. This implies a greater weakening of the hydroxyl (O-H) and (N-H) bonds in each of the urea derivatives than in the thiourea derivatives. These results further show that thiourea and hydroxythiourea are the most antioxidant of the six molecules

From these analyses, it appears that the replacement of the oxygen atom by that of sulfur considerably modifies the antioxidant properties of the urea molecule

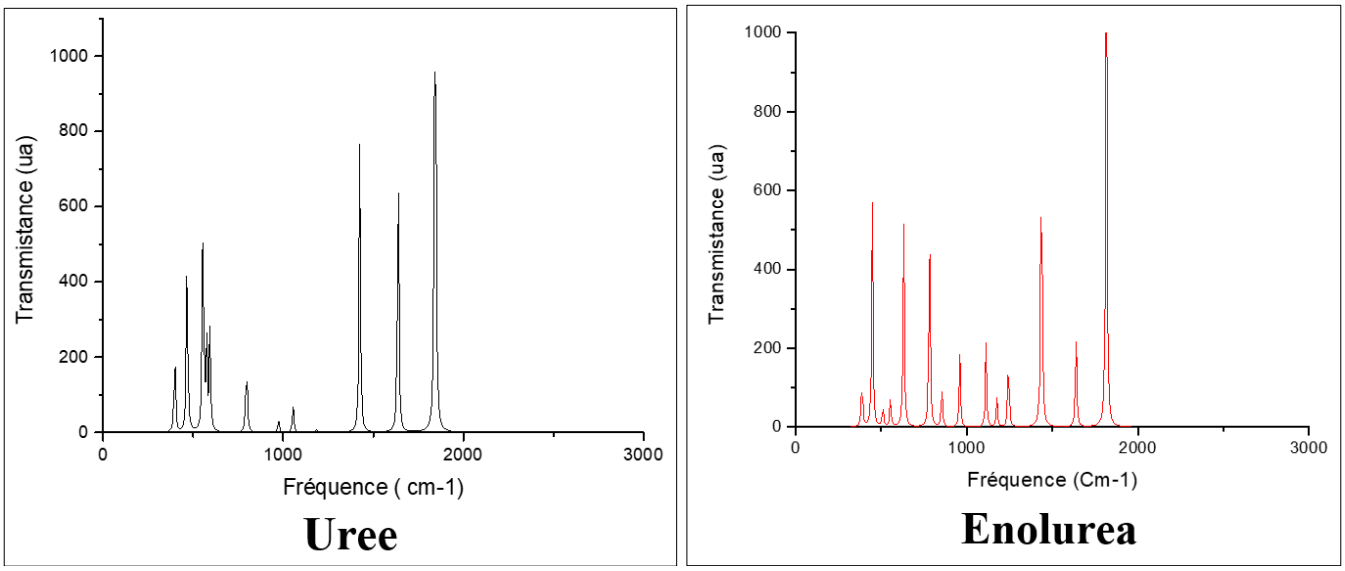

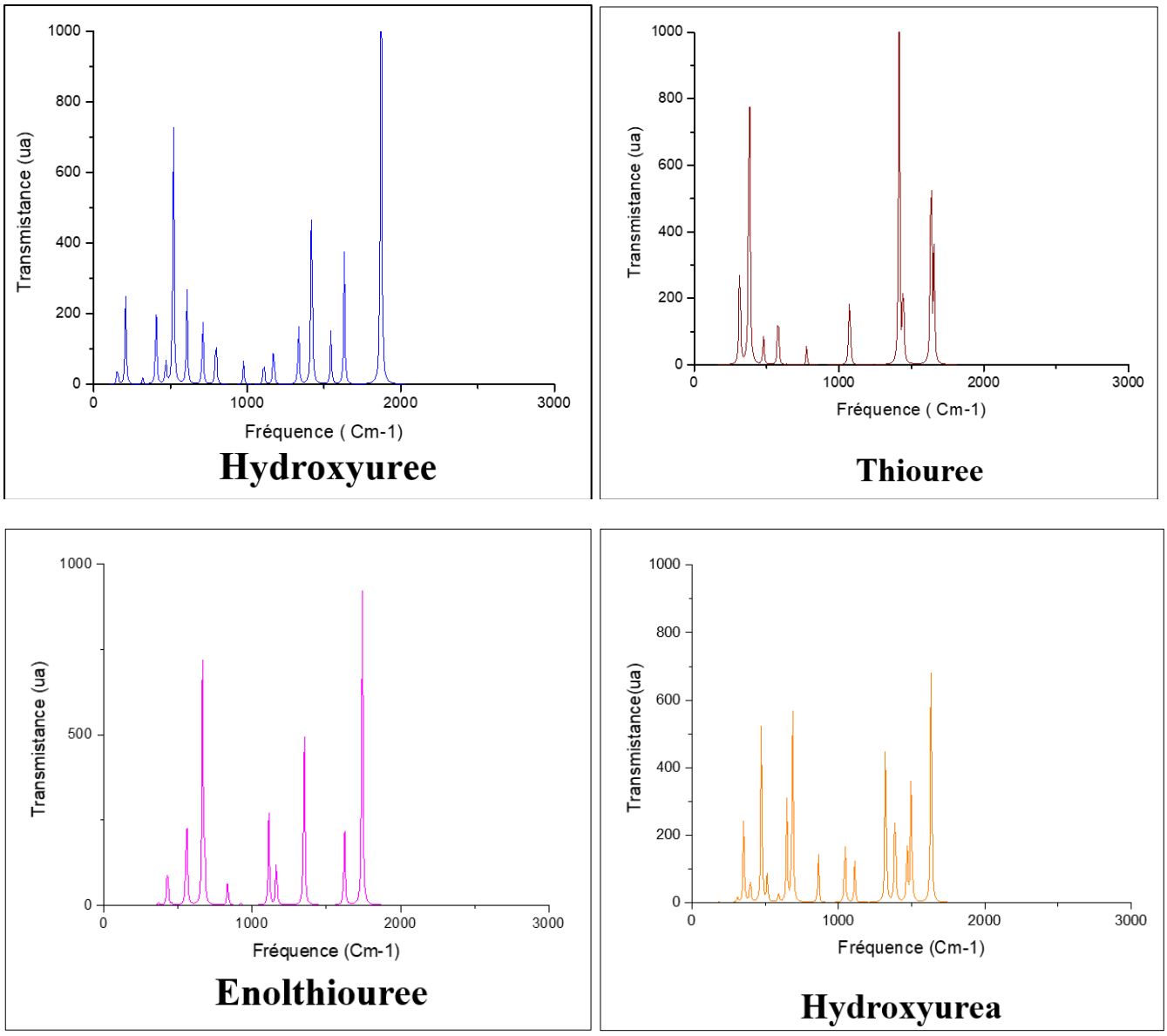

Fig 3: Infrared spectra of urea, Enolurea, thiourea, hydroxyurea, hydroxythiourea and enolthiourea

Representation of the molecular electrostatic potentials in three dimensions (3D) of each molecule

The electron populations at the potential energy surface are indicated by different colors. The 3D representation of the potential energy surfaces of urea, Enolurea, thiourea, 1-hydroxyurea, hydroxythiourea and enolthiourea were shown (Figure 4). The analysis of the different surfaces showed that the electron density values increase in the following order: Red > Orange > Yellow > Black > Blue

For urea, Enolurea, hydroxyurea, the electron density is in the regions between [-3.780 ua; 3.780 ua], [-3.560 ua; 3.460 ua] and [-4.700 ua; 3.500 ua] respectively. The analysis of the molecular electrostatic potentials (MEP) of each of these three molecules shows that they possess more electron-rich partial negative charges (electrophilic site) than electron-deficient charges (nucleophilic site); which means that these three molecules are good antioxidant candidates. Moreover, of the three molecules, enolthiourea presents a stronger electronic delocalization; this molecule thus appears to be the most antioxidant of the three molecules.

For thiourea, hydroxythiourea and enolthiourea, the electron density is in the regions between [-3,800 ua; 3,800 ua], [-3,820 ua; 3,450 ua] and [-5,020 ua; 3,120 ua] respectively. The analysis of the molecular electrostatic potentials (MEP) of each of these three molecules shows that there is more electrophilic site than nucleophilic site; which means that these three molecules are good antioxidant candidates. Moreover, thiourea and hydroxythiourea presented more electrophilic sites. This result indicates that these two molecules are the most antioxidant.

A comparative study of the isoelectric surfaces shows that among the six molecules (urea, Enolurea, thiourea, hydroxyurea, hydroxythiourea and enolthiourea), thiourea and hydroxythiourea have presented the highest electronic populations. From this analysis, it appears that thiourea and hydroxythiourea are the most antioxidant of the six molecules.

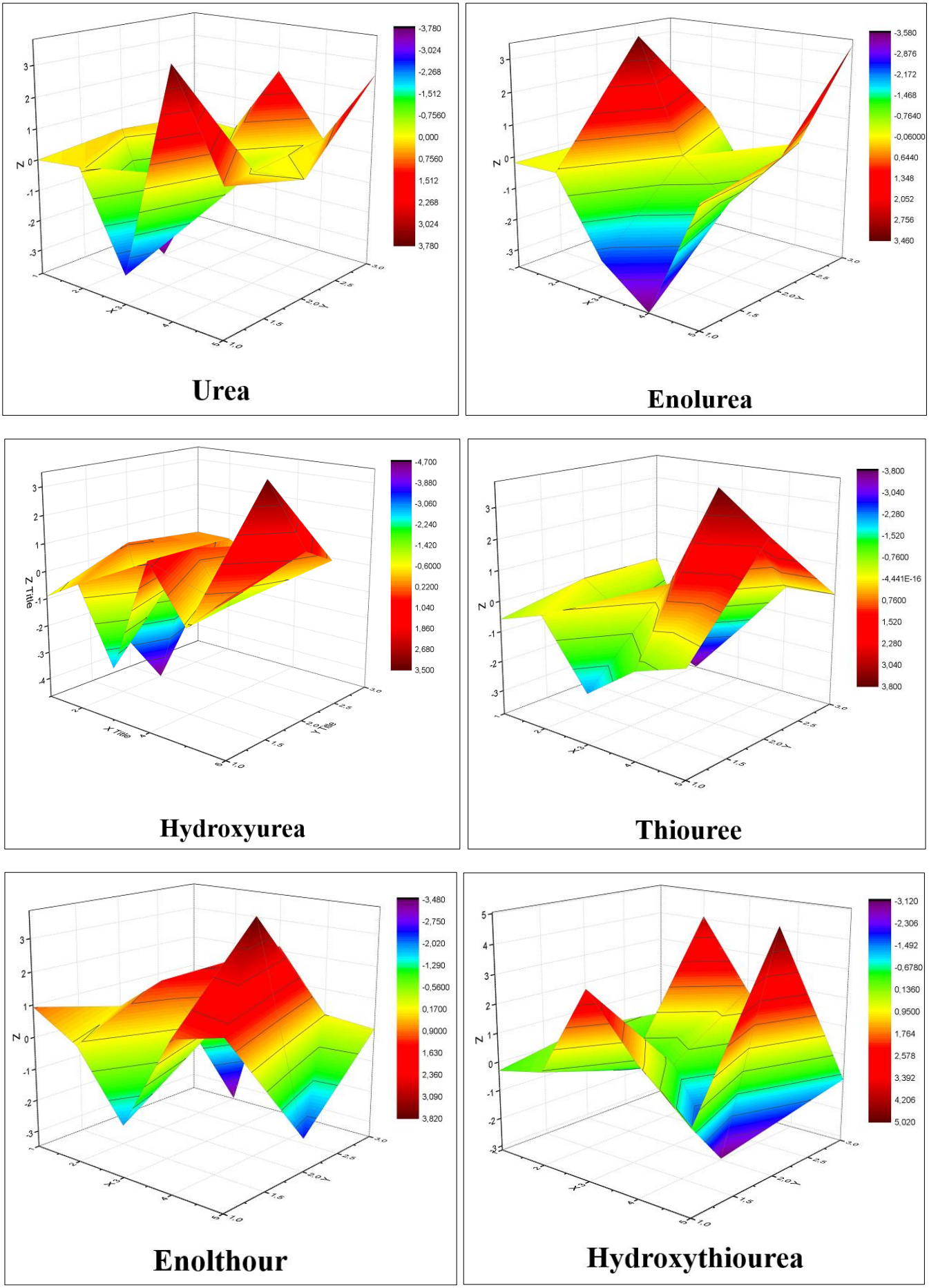

Fig 4: representation of the molecular electrostatic potentials at the 3D level of urea, Enolurea, thiourea, hydroxyurea, hydroxythiourea and enolthiourea

Conclusion

A theoretical study of the chemical reactivities of urea, Enolurea, thiourea, hydroxyurea, hydroxythiourea and enolthiourea, by the method M06-2X/6-311++G (d, p). The comparison between the calculated values of the different electronic, thermodynamic and spectroscopic parameters allowed:

- To identify the oxygen atoms of the O-H groups[8], O-H[9], O-H[7] and O-H[8], as the most important sites for the manifestation of the antioxidant activity of hydroxythiourea, hydroxyurea, enolthiourea and Enolurea respectively.
- That thiourea and hydroxythiourea are the most antioxidant of the six molecules.
- to note that the replacement of the oxygen atom by that of sulfur considerably modifies the antioxidant properties of the urea molecule.
- to note that the mechanism passing by the elimination of atomic hydrogen by homolytic rupture of bond (HAT), as the most probable for the trapping of a radical by each of the molecules.

Regarding the prediction of the antioxidant properties of the molecule and the studied complexes, the theoretical results are in agreement with the experimental data published in the literature.

References

1. Apak R, Ozyürek M, Güçlü K, Çapanoglu E. Antioxidant activity/capacity measurement. 2. Hydrogen atom transfer (HAT)-based, mixed-mode (electron transfer (ET)/HAT), and lipid peroxidation assays. Journal of agricultural and food chemistry. 2016;64(5):1028-1045.
2. A DFT. study on the addition and abstraction; Mwadham. M. Kabanda & Kemoabetswe R. N. reactions of thiourea with hydroxyl radical Serobatse, Journal of Sulfur Chemistry; c2017. https://doi.org/10.1080/17415993.2017.1359269
3. Saha SK, Chandrakanth RC, Krishnamurthy HR. Phys Rev B. 2009;80:15541.
4. Bao BY, Ting HJ, Hsu JW, Lee YF. Protective role of la, 25-dihydroxyvitamin D3 against oxidative stress in non-malignant human prostate epithelial cells. International Journal of Cancer. 2008;122(12):2699-2706.
5. Li JW, Liu YY, Xie LH, Shang JZ, Qian Y, Yi MD, *et al*. Phys Chem. 2015;17:491.
6. Chan B, Gilbert ATB, Gill PMW, *et al*. Performance of density functional theory procedures for the calculation of proton-exchange barriers: unusual behavior of M06-type functionals. J Chem Theory Comput. 2014;10(9):3777-3783.
7. Hameed SA, Alrouby SK, Hilal R. Design of molecular switching and signalling based on proton transfer in 2-hydroxy Schiff bases: A computational study. J Mol Model. 2013 Feb;19:559-569.
8. Vandeputte AG, Sabbe MK, Reyniers MF, *et al*. Theoretical study of the thermodynamics and kinetics of hydrogen abstractions from hydrocarbons. J Phys Chem A. 2007;111(46):11771-11786.
9. Carocho M, Ferre Ira 1C. A review on antioxidants, pro-oxidants and related controversy: Natural and synthetic compounds, screening and analysis methodologies and future perspectives. Food and Chemical Toxicology. 2013;51:15-25.
10. Aquilano K, Baldelli S, Ciriolo MR. Glutathione: New roles in redox signalling for an old antioxidant. Frontiers in pharmacology; c2014. p. 5.
11. Battault S, Whiting SJ, Peltier SL, Sadrin S, Gerber G, Maixent JM. Vitamin D metabolism, functions and needs: from science to health claims. European Journal of Nutrition. 2013 Mar;52:429-441.
12. Caillet S, Côté J, Do Yon G, Sylvain JF, Lacroix M. Antioxidant and antiradical properties of cranberry juice and extracts. Food Research International. 2011;44(5):1408-1413.
13. Ke Y, Qian ZM. Iron misregulation in the brain: a primary cause of neurodegenerative disorders. The Lancet Neurology. 2003;2(4):246-253.
14. Leopoldini Russo N, Chiodo S, Toscano M. J. Agric. Food Chem. 2006;54(17):6343-6351.
15. Morrel Cohen H, Adam W. Journal of Statistical Physics, Hardness and Electronegativity Equalization in Chemical Reactivity Theory; c2006.
16. Kabanda MM, Mammino L. The conformational preferences of acylphloroglucinols – a promising class of biologically active compounds. Int J Quantum Chem. 2012;112(23):3691-3702
17. Kabanda MM, Ebenso EE. Structures, stabilization energies, and binding energies of quinoxaline---(H2O)n, quinoxaline dimer, and quinoxaline---Cu complexes: A theoretical study. J Phys ChemA. 2013;117(7):1583-1595.
18. Kim S, Kuroki S, Ando I. Delusional behavior of n-para±ns with various chain lengths in urea adduct channels by pulsed ¯eld-gradient spin-echo NMR spectroscopy, Chem Phys. 2006;323(2-3):545-552.
19. Accelrys Software Inc, Materials Studio 7.0, Accelrys Software Inc, San Diego; c2014.
20. Carocho M, Ferre Ira 1C. A review on antioxidants, pro-oxidants and related controversy: natural and synthetic compounds, screening and analysis methodologies and future perspectives. Food and Chemical Toxicology. 2013 Jan 1;51:15-25.
21. Lee S, Kariuki BM, Harris KDM. Hydrogen-bonded chains of - diaminoalkane and,!-dihydroxyalkane guest molecules lead to disrupted tunnel structures in urea inclusion compounds, New J Chem. 2005;29(10):1266-1271.
22. Lu T, Chen F. Multiwfn: A multifunctional wave function analyzer. Journal of computational chemistry. 2012 Feb 15;33(5):580-92.
23. Reinboth M, Wolffram S, Abraham G, Ungemach FR, Cermak R. Oral bioavailability of quercetin from different quercetin glycosides in dogs. British Journal of Nutrition. 2010 Jul;104(2):198-203.
24. Hara Y, Jovanovic SV, Steenken S, Simic MG. J. Chem. Soc. Perkin Trans. 2001;2:2497-2504.

Journal of Research in Chemistry

E-ISSN: 2709-9423
P-ISSN: 2709-9415
JRC 2023; 4(1): 39-46

www.chemistryjournal.net
Received: 12-11-2022
Accepted: 18-12-2022

R Chabi Doco
Laboratory of Theoretical Chemistry and Molecular Spectroscopy (LACTHESMO), Faculty of Sciences and Techniques (FAST), University of Abomey–Calavi (UAC); 03 BP 3409 Cotonou, Benin

MTA Kpota Houngue
Laboratory of Theoretical Chemistry and Molecular Spectroscopy (LACTHESMO), Faculty of Sciences and Techniques (FAST), University of Abomey–Calavi (UAC); 03 BP 3409 Cotonou, Benin

Urbain A Kuevi
Laboratory of Theoretical Chemistry and Molecular Spectroscopy (LACTHESMO), Faculty of Sciences and Techniques (FAST), University of Abomey–Calavi (UAC); 03 BP 3409 Cotonou, Benin

YGS Atohoun
Laboratory of Theoretical Chemistry and Molecular Spectroscopy (LACTHESMO), Faculty of Sciences and Techniques (FAST), University of Abomey–Calavi (UAC); 03 BP 3409 Cotonou, Benin

Correspondence
R Chabi Doco
Laboratory of Theoretical Chemistry and Molecular Spectroscopy (LACTHESMO), Faculty of Sciences and Techniques (FAST), University of Abomey–Calavi (UAC); 03 BP 3409 Cotonou, Benin

Physicochemical modeling of myricetin complexes by Zinc II ions

R Chabi Doco, MTA Kpota Houngue, Urbain A Kuevi and YGS Atohoun

Abstract
Myricetin is phenolic compound, commonly found in vegetable kingdom (fruits, vegetables, roots etc.) and an integral part of daily diet of humans. Several experimental and theoretical works have shown that this molecule has an important antioxidant power.
Indeed, since the discovery of relationship between antioxidant activity of certain phenolic compounds and their ability to chelate metal ions, many experimental studies devoted to complexation of molecules such as quercetin, myricetin, kaempferol, rutin, morine with various metals (Cobalt, Nickel, Zinc, Copper, Molybdenum, Europium) were realized. However, these experimental studies do not yet constitute a standard means of determining complexation sites of molecules.
In present work, study of complexation of myricetin by Zn^{2+} ion was carried out by Hatree-Fock method, and in 6-311G (d, p) base set. The results of various calculations made it possible to:

- release hydroxyl groups as myricetin complexation sites;
- note that the complexes obtained are more antioxidants than myricetin;
- show that the complexation of myricetin causes bathochromic shifts of absorption bands.

Keywords: Hatree-fock, myricetin, complexe, antioxidant

Introduction
The ability of phenolic compounds to form complexes with metals (Iron, Magnesium, Aluminum, Copper, Zinc.) by process of chelation has long been used for analytical purposes, especially for revelation of chromatograms and for determination of these substances (Crichton *et al*., 2001) [2]. Today, thanks to their complexing properties, flavonoids are used to detect the presence of metal ions such as iron, Zirconium, Antimony (Pierre and *al*., 2002) [15]. It has long been known that phenomenon of complexation plays the most important role in the coloration of plants and, studies have shown that the ability of flavonoids to inhibit the growth and development of certain insects stem from their complexing properties (Tapiero and *et al*., 2001) [18].
Antioxidant activity of flavonoids is related to this ability to complex metals. These molecules can trap free radicals responsible for oxidation by complexing catalyst metal ions of the formation reaction of these radicals (Ke & Qian, 2003) [11]. Indeed, since the discovery of relationship between activity of certain flavonoids and their ability to chelate metal ions, many studies are devoted to complexation of molecules such as quercetin, rutin, morine with various metals, Cobalt, Nickel, Copper, Molybdenum, Europium (Chaves and *et al*., 2007) [3] have been realized.
Several theoretical and experimental work on flavonoid coordination properties have been published in literature and often contradictory results have been obtained with regard to metal/ligand binding site.
Experimentally, for example, studies have shown that these contradictions are due to the variation of conditions in study environments. Indeed, it is generally accepted that in alkaline solutions, the Fe^{3+}, Cu^{2+}, Zn^{2+} and Al^{3+} ions have the highest affinity for ortho-dihydroxyl group of quercetin (Y. Hara and *al*., 2001, Maria M. Kasprzak *et al*., 2005) [20, 25]. The study in acid solution of different chelation sites of quercetin in the presence of iron has shown that catechol group remains the main chelation site of Fe (J. Cui and *et al*., 2013) [9]. In the same year, Dimitric Markovic and *al.* presented data that corroborated opposite (Y. Hara, 2001) [20]. They reported the formation of Fe-quercetin complex in an acidic solution, with coordination via sites 3-4 or 4-5 (Figure 1), whereas for a high pH solution, the binding of Fe

to the catechol group was advocated. For different solvents used for fisetin, these same authors also observed the formation of a fisetin-Fe complex involving coordination via the 3-4 site. The reduction of Fe^{3+} to Fe^{2+} by fisetine at acidic pH has also been described, while at higher pH, Fe^{3+} and Fe^{2+} complexes coexist.

On theoretical side, several authors using DFT methods have shown that Cr^{3+} ions promote the deprotonation of the 4-5 sites of quercetin and luteolin (Maria M. Kasprzak *et al*., 2005, Jun Ren and *et al*., 2007). [21, 25], whereas Pb^{2+} ions bind preferentially to the 3'-4 site of each of these molecules (Katiyar Santosh K, *et al*., 2008) [22]. Other theoretical studies published in the literature have reached the same conclusions (M. Leopoldini and *al*., 2006) [12]. Also in 2012, Y. Zhang and *al.* performed a DFT study on quercetin complexes with aluminum. They indicated that there is difference between chelation sites of the solid state and those in solution. For their part, in 2013 by the DFT/B3LYP/6-31G method (2df, 3dp), by studying the UV-vis and IR spectra of luteolin complexes with Cadnium II, SONG Liao and *al.* Have shown that the chelation sites of this molecule are those of catechol par.

Of all foregoing, it should be noted that to our knowledge, no theoretical work with respect to the chelation sites of myricetin by Zn^{2+} has yet been performed. Indeed, several experimental works (Ez-zohra NKHILI; thesis 2009) [5] and theoretical (Chabi and *al*., 2018) [23] have shown that this molecule has very important antioxidant power.

The objective of the present work is to determine the best antioxidant among the complexes of the myricetin by methods of quantum chemistry. The reactivities of different chelation sites will be compared with each other, in order to deduce the preferential sites for reinforcing antioxidant capacities of this molecule. To achieve this objective, various electronic and spectroscopic parameters will be calculated and the results will allow to deduce a ranking order of the antioxidant powers of each complexes as well as the most appropriate chelation sites for this molecule.

Materials and Methodology

Materials

Chemical systems in our study were myricetin and complexes obtained from myricetin and the Zn2+ ion provided by zinc chloride ($ZnCl_2$)

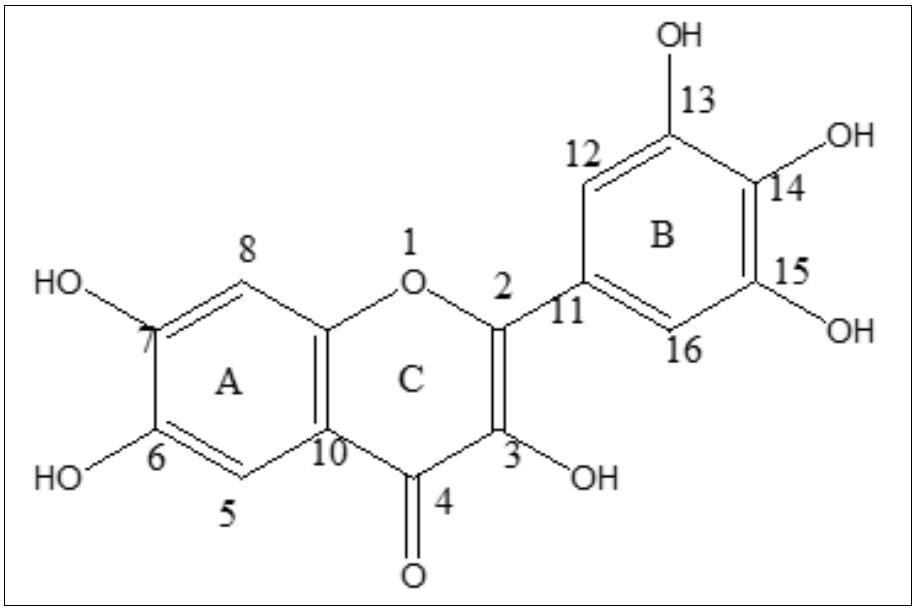

Fig 1: Représentation spatiale de la myricétine

Methodology

For myricetin and each complex, calculated parameters were:

- **Structural parameters**

For molecule with several degrees of freedom, potential energy surface is hyper-surface with several minima and maxima. The maxima correspond to transition states and the minima to equilibrium geometries or conformations of molecule. In a state of minimal energy, vibration frequencies of molecule are all positive. The lowest of minima called global minimum, represents the most stable conformation of studied system.

Each of compound was studied by Hatree-Fock method in the 6-311G (d, p) atomic orbital base. At the beginning of the complexation process, $ZnCl_2$ molecule was placed about 2,50 Å of each of hydroxyl groups considered.

Electronic parameters

$$Gap_{(\mathrm{HOMO-LUMO})} = ELUMO - EHOMO,$$

which is weaker as molecule has a high antioxidant power

- **Hardness (η)** which expresses the resistance of molecule to the change of its number of electrons or to charge transfer (Bonin KD and *al*., 1997). The harder the hardness, less reactive the molecule is:

$$\eta = \frac{(\mathrm{ELUMO} - \mathrm{EHOMO})}{2}$$

- **Electronegativity (χ),** which measures tendency of chemical species to attract electrons (Morrel H., 2006) [13]:

$$\chi = -\frac{(ELUMO + EHOMO)}{2}$$

- **Electrophilic index (ω),** which represents the stabilizing energy of molecule saturated by electrons from its surroundings (Payan-Gomez and *al*., 2010):

$$\omega = \frac{\chi^2}{2\eta}$$

- **Electrofugacity**, which indicates the ability of a compound to donate one or more electrons $\Delta Ee = \omega + I$, *I=-ELUMO* (Ayers and *al*., 2005) [26]
- **Nucleofugacy** that reflects the ability of a compound to accept one or more electrons

$\Delta En = \omega - A$, *A=-EHOMO* (Ayers and *al*., 2005) [26]

Spectroscopic parameters: such as Infra-red spectra and UV-visible spectra were calculated by TD-DFT method. This parameter will allow us to find the influence of complexation of myricetin on antioxidant properties of it.
Calculations were made by Hatree-Fock method in the 6-311G (d, p) atomic orbital Pople base set (J.P. Perdew and *al*., 1996) [24].

Results and Discussions

Study of structural properties of compound

Figures 2, 3, 4, 5 and 6 show optimized geometry of myricetin and each of the complexes obtained from myricetin and Zinc chloride ($ZnCl_2$). The various complexes obtained allow us to make following observations:

- For complex 1, there was formation of bond between O^{14} and Zn metal since the interatomic distance $O^{14}Zn^{34}$ is 1.98 Á, which is in agreement with experimental data published in literature (Symonowicz *et al*., 2012) [17]. The preferred complexation site is thus the O^{14} atom of the $C^8=O^{14}$ group. However, the geometry of the metal in the complex is trigonal rather than tetrahedridic. This observation shows that the complex obtained is unstable.
- For complexes 2, 3 and 4, globally, hydroxyl groups $O^{26}H^{27}$ ((O^{26} ----- Zn^{34}) = 2.21 Å) and $O^{24}H^{25}$ ((O^{24}----- Zn^{34}) = 2.23Å), $O^{32}H^{33}$ ((O^{30}----- Zn^{34}) = 2.20 Å and $O^{26}H^{27}$ ((O^{30} ----- Zn^{34}) = 2.21 Å) of B cycle on one hand and $O^{30}H^{31}$ (O^{30} --- --- Zn^{34}) = 2.12 Å) of C cycle, on other hand are favorable to complexation of myricetin. Geometry of Zinc in these three complexes is tetrahedral which augurs a good complexation and therefore confirms that these hydroxyl sites are true sites of chelation of myricetin. This result is in agreement with experimental results published in literature (Jun Ren and *al*, 2007, Symonowicz and *al*, 2012) [21, 17]. According to these authors, the hydroxyl groups of the catechol part favor the chelation of flavonoids by metal ions.

From these analyzes, it appears that Zinc metal complexes can be obtained from myricetin. However, these results should be compared by calculating the electronic parameters of each of the complexes and myricetin in order to refine the conclusions of the present work.

Analysis of electronic parameters of myricetin and its complexes

For different complexes and myricetin, calculated values of electronic parameters, at Hatree-Fock levels approximation are recorded in table 1:

Table 1: Calculated Values (kJ/mol) of Electronic parameters of Complexes 1, Complex 2, Complex 3, Complex 4 and Myricetin

	E_{HOMO} (kJ/mol)	E_{LUMO} (kJ/mol)	E_{Gap} (kJ/mol)	ω (kJ/mol)	ΔE_e (kJ/mol)	ΔE_n (kJ/mol)
Myricétine	-831.25	157.5	988.75	105	656.25	1023.75
Complexe 1	-866.4	26.25	892.65	5773.36	5198.75	13098.75
Complexe 2	-866.4	78.76	945.16	3491.25	4672.5	2598.75
Complexe 3	-866.4	78.76	945.16	3491.25	4672.5	2598.75
Complexe 4	-787.65	105.02	892.67	5771.36	5196.75	13098.75

Results in Table 1 show that

- All of the four complexes gave, on the one hand, Gap (HOMO-LUMO) lower than of myricetin and on the other hand electrophilic index (ω) values higher than that of myricetin. These series of results, in agreement with experimental data published in literature, mean that the complexes are very stable and therefore more antioxidant than myricetin (CHERRAK Sabri Ahmed, Thesis 2017) [4]. Zinc II ion would then enhance antioxidant capacity of myricetin. Overall, the ranking order of the Gaps of the four complexes would be: Complex 1 <complex 4 <complex 2 ≈ complex 3.
  Antioxidant activity of complexes 1 and 4 would therefore be greater than that of complexes 2 and 3.
- Of the four complexes, the highest values of electrofugacity (ΔEe), nucleofugacy
  (ΔEn) and electrophile index (ω) were obtained by complexes 1 and 4. This result indicates that these complexes are more antioxidants than complexes 2 and 3.
  These analyzes show that complexes resulting from the chelation of myricetin with Zn II ion are more antioxidant than myricetin. Also, complexes 1 and 4 possess the highest antioxidant powers of the four complexes

Representation of HOMO-LUMO energies and iso surface of myricetin and each complex

For myricetin and each of the complexes 1, 2, 3 and 4, energies HOMO, LUMO and iso surface have been represented in figure 2, 3, 4,5 and 6.
Analysis of these different figures reveals that:

- For myricetin, HOMO and LUMO are distributed along all three cycles (A, B and C), whereas for all four complexes these orbitals are distributed over the cycles (B and C). This result indicates that presence of Zn II ion modifies the distribution of electron cloud at level of myricetin; this promotes a high electron density at these two cycles. This implies an increase in antioxidant power.

- The representation of potential energy surface of each of complexes, shows globally, that areas of high electron density are at $C^{8}O^{14}$, $O^{26}H^{27}$, $O^{24}H^{25}$, $O^{32}H^{33}$, $O^{26}H^{27}$ and $O^{30}H^{31}$ groups. This distribution of electron density, due to the presence of Zn II ion made it possible to draw the same conclusions as above. The sites favorable for complexation of myricetin by Zn II ion are Oxygene (O) atom of $C^{8}O^{14}$, $O^{26}H^{27}$, $O^{24}H^{25}$, $O^{32}H^{33}$, $O^{26}H^{27}$ and $O^{30}H^{31}$ groups.

Influence of complexation on UV-vis spectra of myricetin

The absorption curves of UV-Visible spectrum of myricetin and complexes 1, 2, 3, 4 were calculated and represented at HF/6-311G (d, p) level (Figure 6). From analysis of different absorption curves it follows that:

- Complex 1, has five (05) UV-screw absorption peaks whose absorption waveband varies from 100 to 350 nm. With regard to complexes 2, 3 and 4, they have 4 peaks and absorption wavelengths are between 50 nm and 300 nm. On other hand, Myricetin has 4 absorption peaks less hypertrophied than those of the four complexes and the length of the absorption band is between 98nm and 300nm. From these analyzes, it appears that, the presence of Zn II ion, It has strengthened electronic delocalization of myricetin. This result indicates that each of the four complexes has broader range of UV-visible spectrum than myricetin. It follows that complexes 1, 2, 3 and 4 are more antioxidant than myricetin. the complex 1 having presented wider range of absorption band compared to other complexes, thus appears the most antioxidant of the 4 complexes. Indeed, according to the experimental work published in literature by Ez-zohra NKHILI in 2009 [5], molecules with wide range of UV-vis spectra facilitate electronic delocalisation and have a strong antioxidant character.
- Comparison between UV-visible absorption spectra of complexes revealed that of the four, complexes 2, 3 and 4 showed the same absorption curves with almost the same number of peaks. Which means that these complexes possess very close antioxidant powers.

From all above, it can be concluded that complexation of myricetin by Zinc II ions causes bathochromic displacements of the absorption bands of myricetin and increases antioxidant power thereof. This behavior is observed especially with complex 1.

Analysis of Infra-Red Spectra of Myricetin and Complexes 1, 2, 3 and 4

Infra Red (IR) spectra of myricetin and each of 4 complexes are shown in Figures 2, 3, 4,5 and 6 below. From analysis of different spectra, it appears that:

- Infra-red spectra of myricetin and its complexed forms are dominated by bands in spectral range 0-4.200 cm^{-1}.
- Significant frequency changes around the spectral band between 4000 cm^{-1} and 4250 cm^{-1} are observed between the IR spectra of myricetin and that of the complexes. This observation between IR spectra indicates that chelation causes very important structural variations in myricetin. This result is in agreement with the experimental results published by Laurence VRIEL YNCK in 1996.
- IR spectra of complexes 1, 2, 3 and 4 gave less intense bands than those of myricetin. This result indicates that electronic offshoring is more important at level of complexes than myricetin. This implies a weakening of the hydroxyl (OH) bonds at the level of each of the complexes. Complexes 1, 2, 3 and 4 therefore appear to be more stable than myricetin. The Zn II ion strengthens the antioxidant power of myricetin.
- IR bands from 0 to 2000 cm^{-1} are virtually identical for myricetin and each of 4 complexes. On other hand, for band at 4000 cm^{-1} and 4250 cm^{-1}, we have difference between different peaks observed. By comparing this spectral band for the ligand (myricetin), and complexes 1, 2, 3 and 4, it is found that complexation peaks are obtained practically at level of band at 4150 cm^{-1}. These peaks corresponding to peak of the coordination link.

From these results, it follows that Zinc II ion modifies structural properties and increases the antioxidant activity of myricetin

The structure of Zinc in Complex 1 has a trigonal geometry. However, this complex has good antioxidant power. It therefore seems interesting to seek and find tetrahedral form by stabilizing it with other ligands for more judicious comparison of antioxidant properties.

Stabilisation of complex 1

Figure 7 shows the complex obtained from Zinc chloride ($ZnCl_2$) and two molecules of myricetin. The distance between groups ($C^{8}O^{14}$, $O^{28}H^{29}$) and $ZnCl_2$ for optimization of geometry is 2.50 Å.

From analysis of results, it appears that:

- Zinc metal structure is tretrahedral in complex (v). This result indicates that ZnII metal complex stabilizes with two molecules of myricetin. The distances (O---Zn) obtained on either side of two ligands being identical and is equal to 2.01 Å, justifies good coordination between Zn II and all the two molecules of myricetin.
- HOMO, LUMO orbitals are distributed along all three cycles (A, B and C) of the ligands. Similarly, the representation of potential energy surface of complex, shows that globally, areas of high electron density are at $C^{8}O^{14}$, $O^{26}H^{27}$, $O^{24}H^{25}$, $O^{32}H^{33}$, $O^{26}H^{27}$ and $O^{30}H^{31}$ (w) groups of this same ligand. around Zn II. This result, identical to that of complex 1, indicates that presence of Zn II ion modifies distribution of electron cloud at the level of myricetin and promotes a strong electronic delocalization at these cycles A, B and C.
- With regard to UV-vis and Infra-red spectra, the results obtained practically coincide with those of complexes 2, 3 and 4, with the difference that UV-vis spectrum of the complex has an absorption band varying from 124 nm to 325 nm. This means that the latter has slightly higher antioxidant power than that of 2,3 and 4 complexes.
- Calculation of energy Gap for the complex 5 gives 866.41 kJ/mol. This value being higher than those of complexes 1, 2, 3 and 4, indicates that the complex 5 would be more antioxidant. This result shows that the formation of complex from two molecules of myricetin further enhances more antioxidant capacity of the latter.

From these results, we can conclude that complex obtained from two molecules of myricetin is much more stable and therefore more antioxidant than complexes formed from a molecule of myricetin.

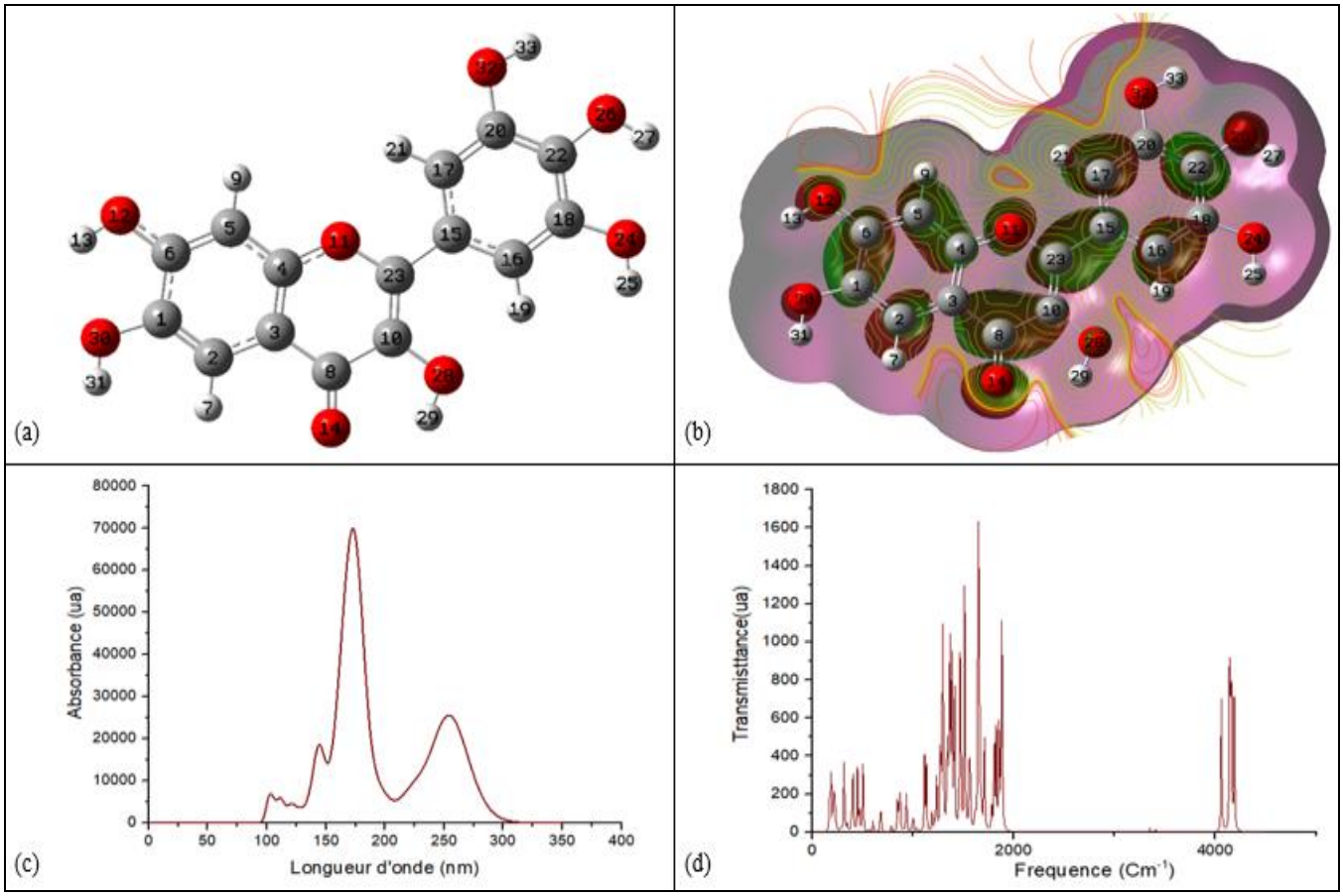

Fig 2: representation of optimized forms (a), HOMO and LUMO and SEP (b) orbitals, UV-vis (c) and IR (d) spectra of myricetin to HF / 6-311G (d, p)s

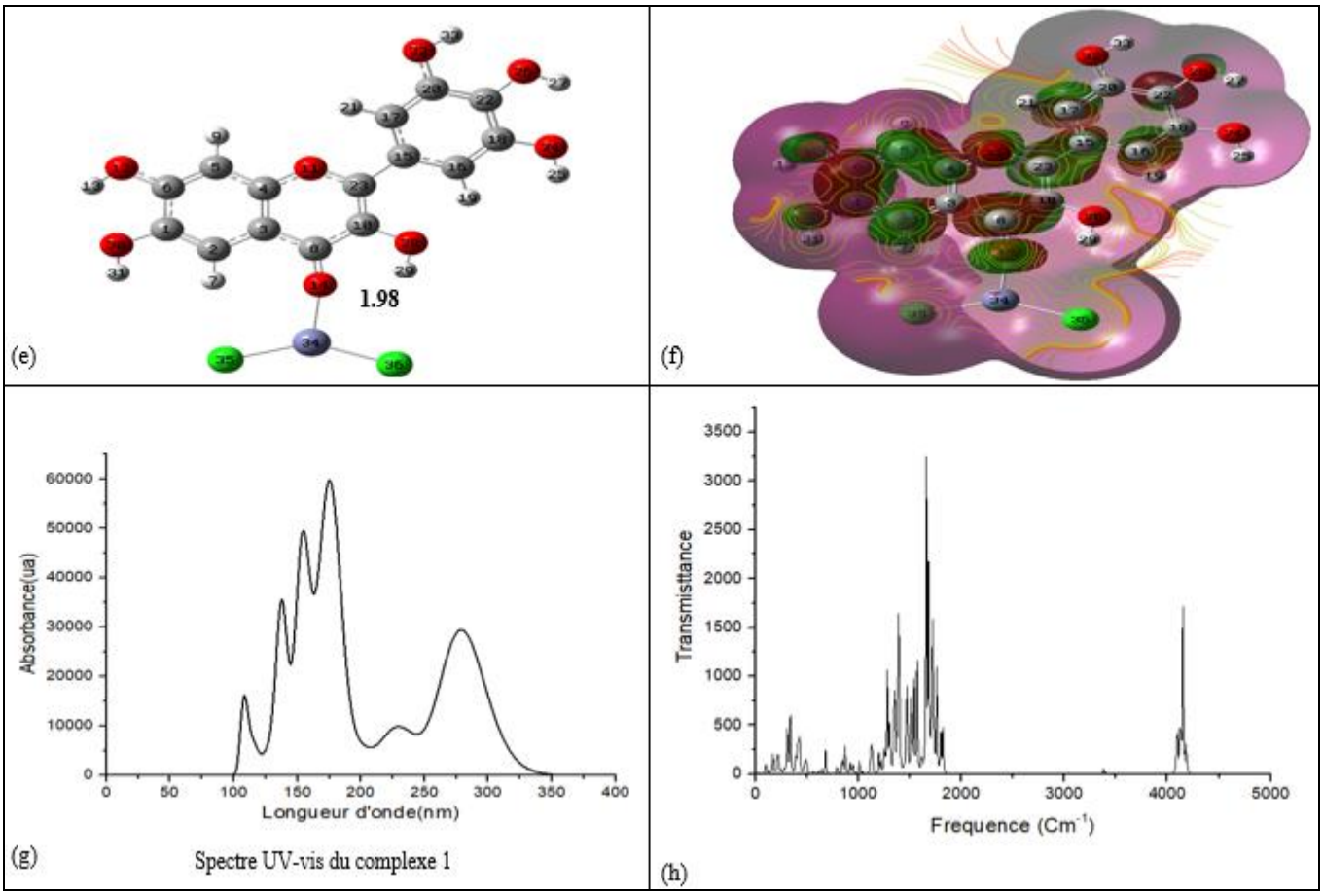

Fig 3: Representation of optimized forms (e), HOMO and LUMO and SEP (f) orbitals, UV-vis (g) and IR (h) spectra of complex 1 to HF / 6-311G (d, p)

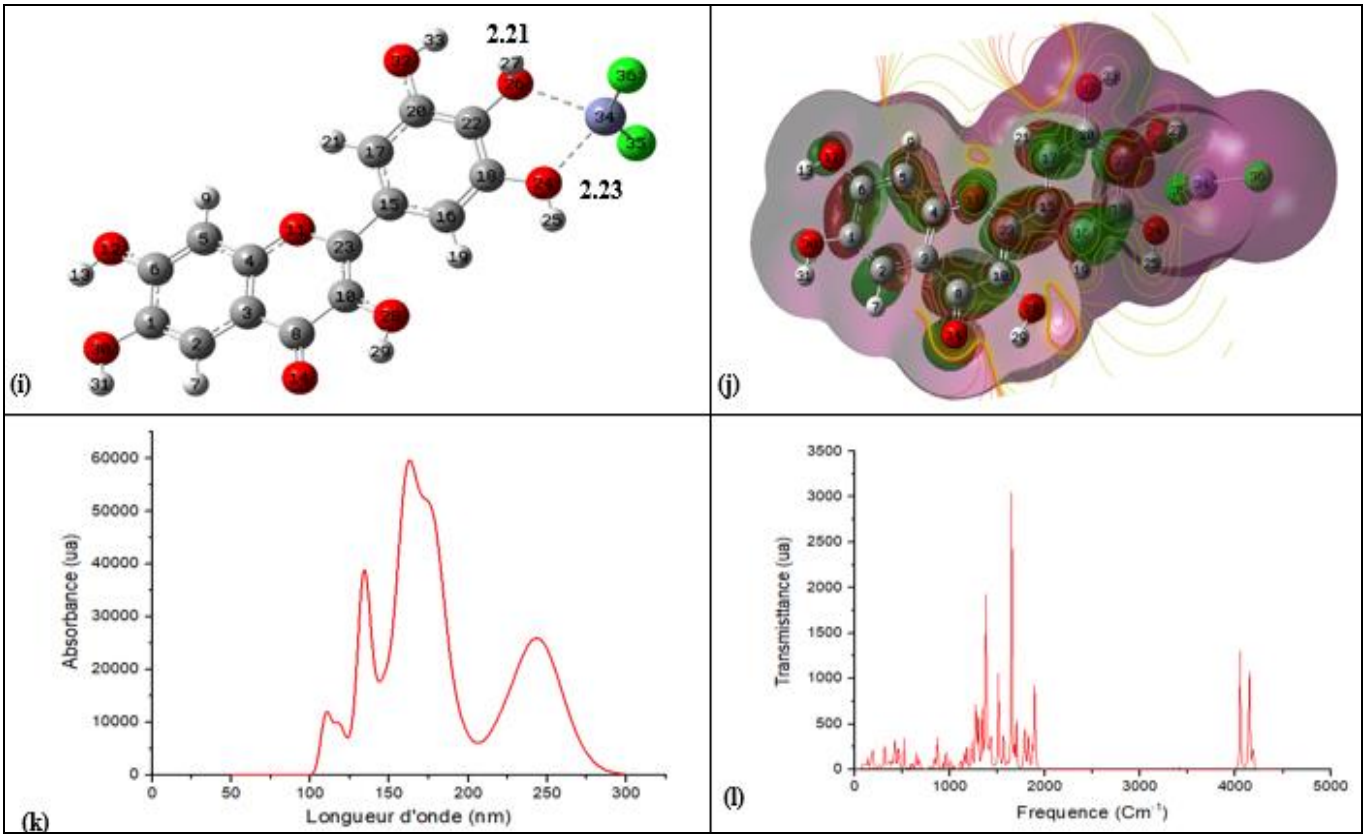

Fig 4: Representation of optimized forms (i), HOMO and LUMO orbitals, SEP (j), UV-vis (k) and IR (1) spectra of complex 2 to HF / 6-311G (d, p)

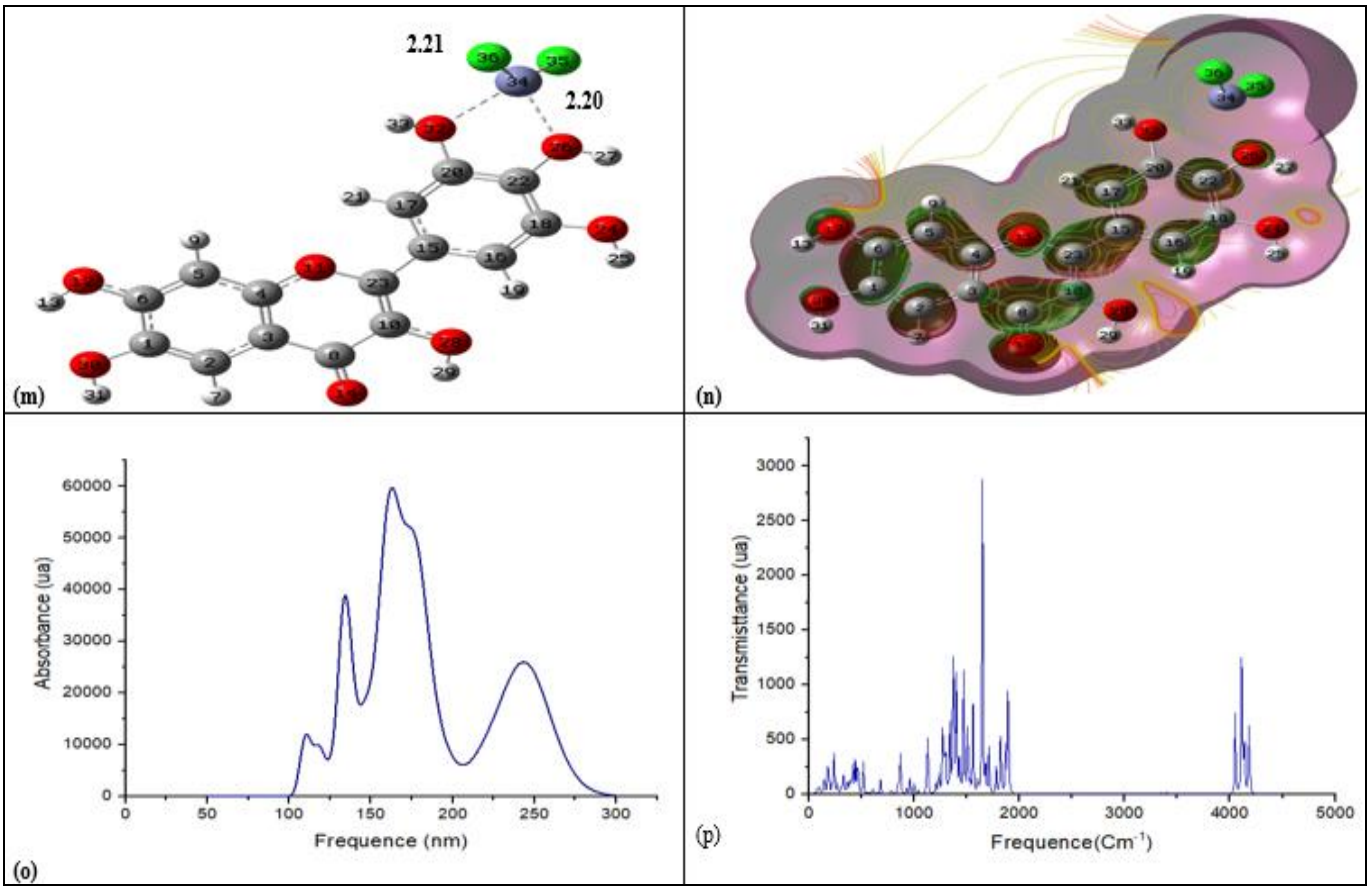

Fig 5: Representation of optimized forms (m), HOMO and LUMO orbitals, SEP (n), UV-vis (o) and IR (p) spectra of complex 3 to HF / 6-311G (d, p)

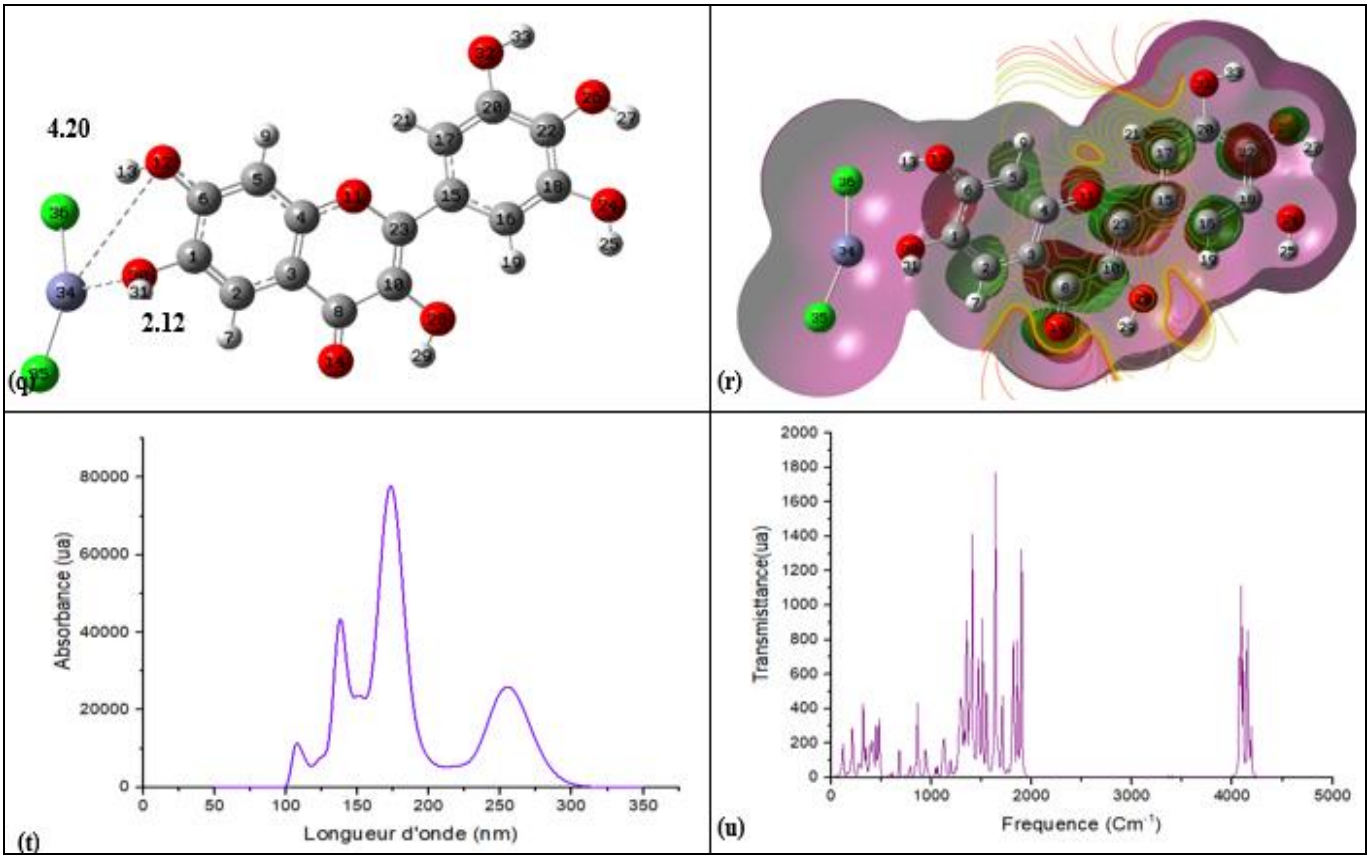

Fig 6: representation of optimized forms (q), HOMO and LUMO orbitals, SEP (r), UV-vis (t) and IR (u) spectra of complex 4 to HF / 6-311G (d, p)

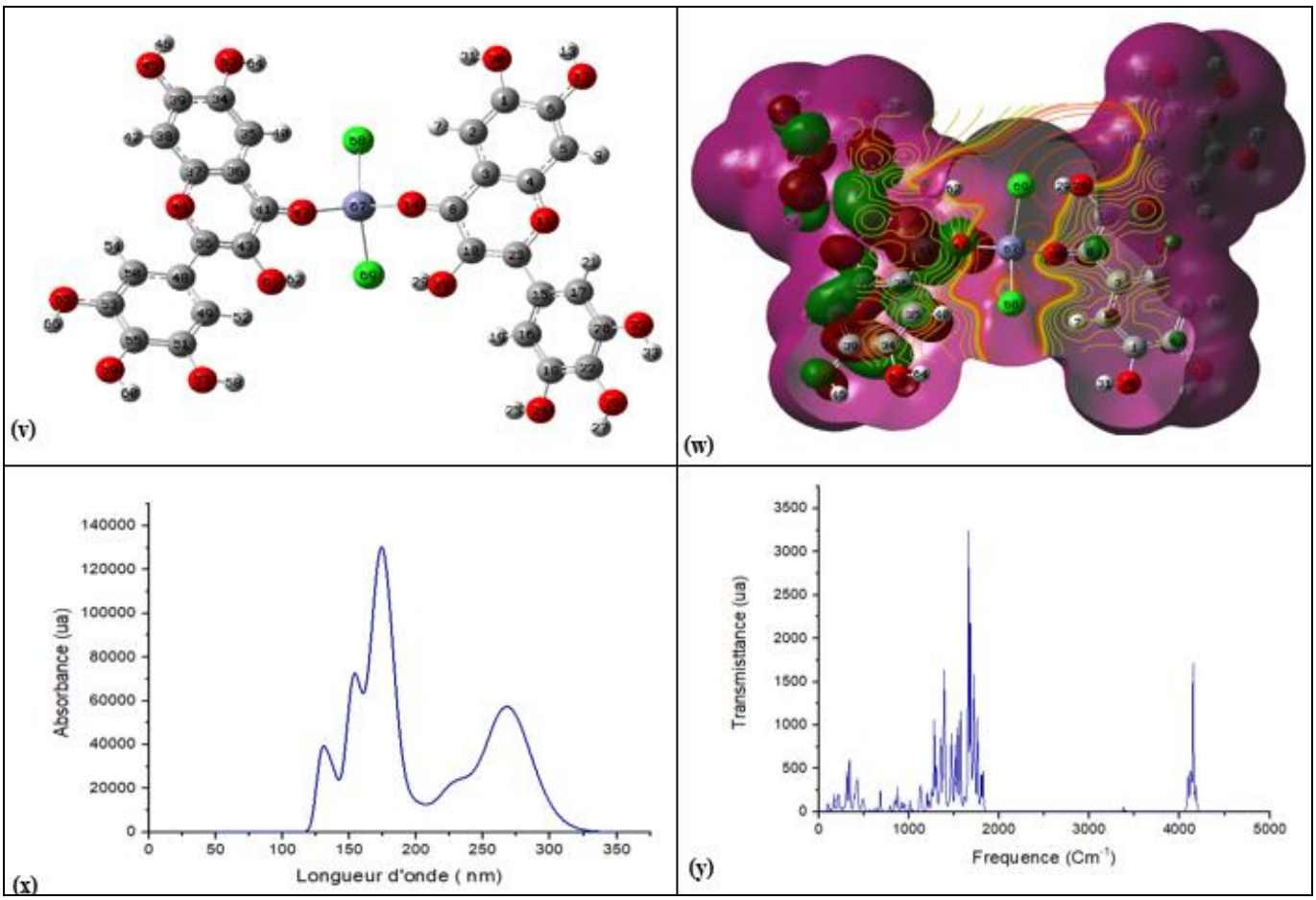

Fig 7: Representation of optimized forms (v), HOMO and LUMO orbitals, SEP (w), UV-vis (x) and IR (y) spectra of complex 5 to HF / 6-311G (d, p)

Conclusion

A theoretical study of chemical reactivities of myricetin and complexed forms was carried out by Hatree-Fock/6-311G (d, p) method. Comparison between calculated values of various structural, electronic and spectroscopic parameters allowed to:

- Release that oxygene (O) atoms of $C^{8}O^{14}$, $O^{26}H^{27}$, $O^{24}H^{25}$, $O^{32}H^{33}$, $O^{26}H^{27}$ and $O^{30}H^{31}$ groups as complexing sites of myricetin
- note that complexes 1, 2, 3 and 4 from myricetin are more antioxidant than myricetin.
- show that complexes 1 and 4 are the most antioxidants of four complexes
- note that complexation of myricetin by Zinc II ions in some cases causes a bathochromic displacement of absorption bands of myricetin.
- show that complex obtained from two molecules of myricetin is more stable and therefore more antioxidant than the complexes formed from molecule of myricetin.

With regard to prediction of antioxidant properties of molecule and the complexes studied, theoretical results are in agreement with the experimental data published in the literature.

References

1. Ayers PW, Levy M. Theor. chem, Acc. 2000;103:353-360.
2. Crichton R, Pierre JL. Old iron, young copper: from Mars to Venus. Biometals. 2001;14(2):99-112.
3. Chaves FJ, Mansego ML, Blesa S, Gonzalez-Albert V, Jiménez J, Tormos MC, *et al*. Inadequate cytoplasmic antioxidant enzymes response contributes to the oxidative stress in human hypertension. American journal of hypertension. 2007;20(1):62-69.
4. Cherrak Sabri Ahmed. Etude *in vitro*. de l'effet antioxydant des complexes Flavonoïdes –Métaux: Relation structure activité; Thèse; c2017.
5. Ez-zohra Nkhili. Polyphénols de l'alimentation: Extraction, Interactions avec les ions du Fer et du Cuivre, Oxydation et Pouvoir antioxydant; Thèse; c2009
6. Payán G, Sergio A, Norma Flores H, Antonino P, Manuel, Piñón M, *et al.* Computational molecular characterization of the flavonoid rutin; Chemistry Central Journal. 2010;4:12.
7. Goitia MT, Montero M, Allan Bulletin. de la Societé Quimica del Peru Femandez Band, B.S. A.L; c1988, 171.
8. Harbome JB. (ed.), Chapman and Hall, London, p. 399.
9. Cui J, Li S. Shaoshun, Mini-Rev. Med. Chem., and refs therein M. 2013;13:1357-1368.
10. Jun Ren, Sheng Meng, Ch. Lekka E, Efthimios Kaxiras. Complexation of Flavonoids with Iron: Structure and Optical Signatures; J Phys. Chem. B. 2008;112(6):1845-1850.
11. Ke Y, Qian ZM. Iron misregulation in the brain: a primary cause of neurodegenerative disorders. The Lancet Neurology. 2003;2(4):246-253.
12. Leopoldini N, Russo S, Chiodo, Toscano M. J Agric. Food Chem. 2006;54(17):6343-6351.
13. Morrel W. Cohen and Adam, Journal of Statistical Physics, Hardness and Electronegativity Equalization in Chemical Reactivity Theory; H; c2006.
14. Maria Kasprzak M. A Andrea Erxlebenc, Justyn Ochockia; Properties and applications of flavonoid metal complexes; The Royal Society of Chemistry J Name. 2013;00:1-3.
15. Pierre J, Fontecave M, Crichton R. Chemistry for an essential biological process: the reduction of ferric iron. Bio metals. 2002;15:341-346.
16. Song Xiao-Li, Gao Li-Geao, Gapo Wei. Chelation betwen luteolin and Cd(II): spectroscopic studies and theorical calculation, chinese journal of inorganique chemistry. 1989-1992;29(9).
17. Symonowicz M, Kolanek M. Flavonoids and their properties to form chelate complexes; c2012.
18. Tapiero H, Gate L, Tew K. Iron: deficiencies and requirements. Biomedicine & pharmacotherapy. 2001;55(6):324-332.
19. Weirong Cai, Yong Chen, Liangli ang Xie, Hong Zhang, Chuny uan Ho. Characterization and density functional theory study of the antioxidant activity of quercetin and its sugar-containing analogues, Eur Food ResTechnol. 2014;238:121-128.
20. Hara Y, Jovanovic SV, Steenken S, Simic MG. J Chem. Soc. Perkin Trans. 2001;2:2497-2504.
21. Ren J, Cheng W, Li S, Suckewer S. A new method for generating ultraintense and ultrashort laser pulses. Nature Physics. 2007 Oct;3(10):732-6.
22. Katiyar SK. Grape seed proanthocyanidines and skin cancer prevention: inhibition of oxidative stress and protection of immune system. Molecular nutrition & food research. 2008 Jun;52(S1):S71-6.
23. Chabi-Jesus C, Ramos-González PL, Tassi AD, Guerra-Peraza O, Kitajima EW, Harakava R, Beserra Jr JE, Salaroli RB, Freitas-Astúa J. Identification and characterization of citrus chlorotic spot virus, a new dichorhavirus associated with citrus leprosis-like symptoms. Plant Disease. 2018 Aug 17;102(8):1588-98.
24. Perdew JP, Burke K, Ernzerhof M. Generalized gradient approximation made simple. Physical review letters. 1996 Oct 28;77(18):3865.
25. Kasprzak MM, Erxleben A, Ochocki J. Properties and applications of flavonoid metal complexes. Rsc Advances. 2015;5(57):45853-77.
26. Effler PV, Pang L, Kitsutani P, Vorndam V, Nakata M, Ayers T, *et al*. Dengue fever, hawaii, 2001–2002. Emerging infectious diseases. 2005 May;11(5):742.